Design, Development and Testing Of an on-line Cosmic Rays Hodoscope

(A study carried out as a part of an international scientific project)

MS. (Electronic Engineering)

Submitted to:

Dr. Ahmed S Syed.

Prepared by:

Waqar Ahmed
MS (Electronics Engineering)
13-FET-06

MS.

539.7223
WAD

1- Cosmic rays.

Abstract

The project is based on on-line study of cosmic rays using cosmic detectors in Hodoscope. Hodoscope have earlier been used for other diverse application, however, the application of Hodoscope for on-line of cosmic rays is being done at CERN and NCP simultaneously for the first time. The aim of project is develop complete hardware setup to communicate with web based software. In this project we have three major modules one is hardware second is the data acquisition system and the third is the web based software modules. In this regard we have carefully designed the working condition of the experiment such as setting up threshold of scintillators, usage of optical grease and generation of fine trigger from the scintillator. We have successfully developed the mode to translate the result online for further use and tested them against the CMS criteria. To meet the criteria of CMS we have designed, developed and calibrated a hodoscope at NCP National Centre for Physics at Islamabad to test RPCs. The End-Cap RPCs meets all the CMS criteria. Therefore they are suitable for the installation in CMS detectors. In order to be able to use the RPCs arranged in the double gap structure on the basis of muon triggering system for the CMS detector all of them must qualify the testing criteria. This is qualified using our developed protocols for online cosmic rays Hodoscope. The CMS criteria tested against our hodoscope is:

- Efficiency should be >= 80 - 95%
- Cluster size should be < 3


- Dark current should be < 5 μA
- Strip occupancy should be < 3 noisy or dead strips

For monitoring dark current and high voltage of the detectors, we control HV power supply and monitor all parameters remotely on web using our developed hodoscope. After testing, they may be shipped to CERN, where they will be installed in the CMS experiment at LHC, which will again run in 2010.

Acknowledgements

In the name of ALLAH, the Most Merciful, Most Gracious, and Benevolent.

First and the foremost, I want to express my immense gratitude to my worthy supervisor Prof. Dr. Ahmed S. Syed for his professional guidance and encouragement throughout this research work. Without his kind and invaluable help, it would have been almost impossible for me to accomplish this job. I am thankful to Director Research Dr Hafeez Hoorani for allowing me to do research in National Centre for Physics (NCP).

Mind is like a parachute. It works only when open and my teachers taught me how to open it. My most profound thanks go to my colleagues, Sajjad Asghar and Sobia and Ashiq Ali for the various bits of knowledge and wisdom, which they imparted to me during different stages of my research work.

Finally, I wish to record my deepest obligation to my parents for their prayers, encouragement and financial support during my studies. Specially, my mother who always loves me and contributes endlessly to keep on the track. No one tolerates me more than she does. I am forever indebted to my brothers and sister for their love and care. A great thanks to all my family for their unconditional support, their trust in me and for keeping me grounded.

Waqar Ahmed

Certificate

It is certified that the work contained in this dissertation was carried out by **Mr. Waqar Ahmed** under my supervision.

(Prof. Dr. Ahmed S. Syed)
Dean Faculty of
Engineering and Technology

Contents

Glossary

NCP	National Centre for Physics
RPC	Resistive Plate Chamber
CERN	European Organization for Nuclear Research
NIM	Nuclear Instrument Modules
PMT	Photo Multiplier Tubes.
TDC	Time to digital converter
ECL	Emitter Coupled Logic
DAQ	Data Acquisition System
VME	Versa module Euro-card
LHC	Large Hadron collider
CAMC	Computer Automated Measurement and Control
JRE	Java runtime engine
CMS	Compact Muon Solenoid
RHIC	Relativistic Heavy Ion Collider
ECAL	Electromagnetic calorimeter
HCAL	Hadron calorimeter
TGCs	
CR	Cathode Rays
ICRS	International Cosmic Ray Service
BEO	Basic environmental observatory
MT	Muon telescope
ADC	Analog to digital converter
TTL	Transistor transistor logic
FEB	Front End Board
GUI	Graphical User Interface
OVC	Over current flow
VETO	
FEC	Front end chips
ASIC	Application Specific Integrated Circuits
SOAP	Simple Object Access Protocol
LVDS	Low Voltage Differential Signal
OPC	
UART	Universal Asynchronous Receiver and Transmitter
FPGA	Field Programmable Gated Array
CMS Collaboration	Compact muon Solenoid collaboration (Different countries scientist involved in this project, part of the project)

Chapter 1

Introduction

1.1 Introduction

Remote laboratories have begun attracting more attention over the last couple of years, however what is really meant by remote laboratories? Remote laboratories are implemented in such away that the student/researcher does not need to be physically present in the lab in order to complete the experiment. Remote labs allow the students/ researcher to interact with the same equipment through an interface which is made available over internet or local network, so that they can work on the experiment as if they are physically working in the laboratory [1]. National centre for physics (NCP), Islamabad had decided to develop remote laboratories by providing services for students in universities and research centers. Our work is focused to develop such facility by carrying out technical research, develop the necessary hardware and finally implement the protocol for application. The research, development and implementation will be carried out at National centre for physics (NCP) Islamabad. The problem area is a direct consequence of research application used in the world frame "Large Hadron collider" experiment at European Organization for Nuclear Research (CERN).

1.2 Objectives of Research

We will develop an on-line hodoscope setup to measure and study dark current for scintillator and Resistive Plate Chambers (RPC) remotely by using web facilities. We also will check efficiency, strip occupancy and cluster size behavior of the detectors (RPC) and check scintillators due to change of high voltage. We aim to assemble sixteen scintillators with guided media and PMT before measurement. After that we will measure efficiency of different eta segments of RPC with the help of small scintillators.

1.3 Project Description

The project is based on on-line study of cosmic rays using cosmic detectors in hodoscope. Hodoscope have earlier been used for other diverse applications, as in the literature [2-27]. However the application of Hodoscope for on-line of cosmic rays is being done at CERN and NCP simultaneously for the first time. The aim of project is to develop complete hardware setup to communicate with web based software. In this project we have three major modules: one is the hardware, second is the data acquisition system and third is the web based software modules.

The hardware module included scintillators and its modules, light guided media and Photo Multiplier Tube (PMT), special purpose Costruzioni Apparecchiature Elettroniche Nucleari (CAEN) nuclear power supply and its modules, Nuclear Instrument Module (NIM) based discriminators and coincidence unit delay unit and RPC (resistive plate chamber) gases detectors.

The data acquisition system for communication with web server I includes MXI-2 NI modules with PCI interface card, Time to digital conversion (TDC) board for study of timing information of RPCs.
The web based software module will be used to communicate with hardware through software using C^{++}.

1.4 Hodoscope

Hodoscope is the combination of detector and nuclear electronics, this setup is used to check the performance of the RPCs detector. The RPC testing area is located in NCP laboratory. The cross-section of each RPC is exposed to cosmic ray muons. Apparatus used for cosmic test included high voltage power supplies, gas flow rate controller, gas mixture, trigger setup and data acquisition system. The hodoscope (cosmic ray muon stand) used in the test can house ten chambers at a time which can be tested simultaneously. The chambers are placed horizontally. Temperature of the laboratory is

kept constant by air-conditioning systems, while humidity and temperature are monitored continuously with the help of proper devices. (Fig 1.1)

The hodoscope consists of scintillators, which are placed at the top and bottom of the Cosmic Ray Muon Stand. These scintillators are 2.0 meters long. To cover the full width of a RPC chamber, we require 8 scintillators on the top and 8 at the bottom, so in total 16 Scintillators are used. The CAEN power supply is used to energies PMT of Scintillator.The trigger is logic based on these scintillators. We are operating these scintillators between 1.0 ~ 1.6KV. Pre-amplifier are used to read out the signals from these scintillators. NIM based module like Discriminator, Coincidence unit are also used to generate trigger of TDCs (time to digital conversion).

Fig. 1.1. Cosmic Setup at National Centre for Physics Islamabad.

1.5 Objectives.

We have develop virtually cosmic setup on Web Page Power supply of the system operate remotely and view the status of tested RPC information like cluster size, strip occupancy, efficiency of the detectors. The student gets the same education and experiment as from attending and completing a laboratory session. Students implementing a web-enabled laboratory experiments instead of having to deal with over crowded laboratory rooms and students rushing to get the work done, in future they will be able to remotely complete the laboratory sessions remotely and at their own pace.

There are three main parts of the system, the Web Interface-Client End and the Web Server Apache, Hodoscope Module and Trigger Logic Module. The Web Server acts the mediator between the Web Interface Client and Hardware Module. The web Interface the graphical user interface which provides the experiment specification is called client. The Web Interface Client is a written in Java script and HTML based which can run on any web browser.

The Lab Server provides the required communication protocols between the Client and Apache Server it is written in AJAX and PHP. The request is received from the Client and the request is sent to the Hardware application.

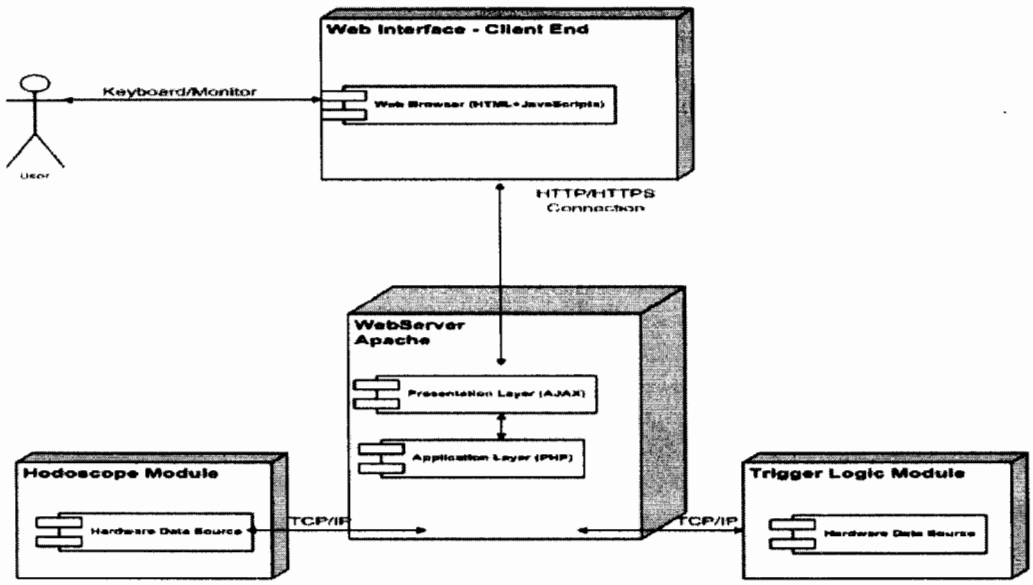

Fig 1.2 Software Deployment Diagram

1.6 Data acquisition system (DAQ)

A DAQ is thought to be equipped with enormous and latest technology of electronics, which meet the different criteria of an experiment and specially designed according to the requirement of an experiment. When all the parts of a DAQ system are combined, then the system is ready to perform the specific applications [27]. Maximum electronics used, in LHC experiment is based on Versa Module Europacard (VME) standards. There are three major parts on which a DAQ system comprises, which are: CAMAC, VME and NIM. These are three different parts,

- **CAMAC (Computer Automated Measurement and Control)**
- **NIM (Nuclear Instrument Modules)**
- **VME (Versa module Euro-card)**

Which are used in many different experiments for data acquisition. They are further divided into many other modules like Time-to-Digital Converter (TDC), scalars, discriminators, amplifiers and many other peripheral devices.

1.7 Detector Analysis

As can be viewed from Fig 1.2 for detector analysis, we require JAVA and client side JAVA run time environment for analysis. The libraries of Java virtual machine and other components are provided by Java Run Time Engine (JRE) to run applets and other application written in the java language [6].

Detector Analysis is a tool, also developed, using java and web services technology in this project. The main feature of data acquisition system is that it provides the users a facility to process data and create plots by sending request to remote servers. Since DAQ online is based on web services technology, it is very easy to do distributed data processing. Data which is received from a RPC is converted into "xml" format using an "xml" conversion tool which is provided with DAQ online. These "xml" files are stored on one of many servers .User can connect any of these servers and then can process the data on them, and can make plots of the processed data. The main feature of this tool is to view strip occupancy chart, strip pie chart, efficiency, timing information and cluster size, etc. [8]

As part of the research methodology, we will use the NCP facilities. Initially a cosmic ray muon test stand was built in the NCP laboratory to test the CMS endcap RPCs. This will be modified further for better performance and efficiency of the hodoscopes. Hodoscope consisting of scintillators will be placed at the top and bottom of the cosmic ray muon stand. These scintillator will be about 2.0 meters long. To cover the full width of a chamber, we aim to place 8 scintillator on the top and 8 at the bottom, so in total 16

scintillator will be used in this experiment. The CAEN power supply will be used to energize PMT of the scintillator. The trigger logic will be based on the design of these scintillators. We aim to operate these scintillators between 1.0-1.6KV for reading out the signals from these scintillators we aim to use preamplifiers based on NIM schemes such as Discriminator and Coincidence units.

The final testing and analysis will be carried out on site at NCP. A specific website will also be developed to run the web-based protocols effectively to ensure the appropriate demonstration of the project.

Chapter 2

Background

2.1 The Large Hadron Collider (LHC)

The LHC is a two-ring machine with a total length of 27 km, which is lies on 100 m below ground between Lake Geneva and the Jura mountains. This will allow the head-on collision of proton beams, each with energy of 7 TeV, and beam collisions of heavy ions, such as lead, with a total center of mass collision energy in of ≈ 1, 250 TeV, which is around thirty times higher than the Relativistic Heavy Ion Collider (RHIC) at the Brookhaven Laboratory in the US[26]. Joint LHC operation could supply electron-proton collisions with a centre-of-mass energy of 7 TeV, some five times higher than that of HERA in the DESY Laboratory, Germany [27]. LHC has enormous potential for research, technology and education. The wide range of possibilities will enable LHC to attain unique place on the frontiers of physics and engineering research.

A TeV is a unit of energy used in high energy particle physics. One eV is the energy gained by a many charge when its moves through potential of one volt. The energy of motion of a flying mosquito is about 1 TeV. The LHC is so extraordinary because it can squeeze the energy into a space which is about a million times smaller than a mosquito [28].

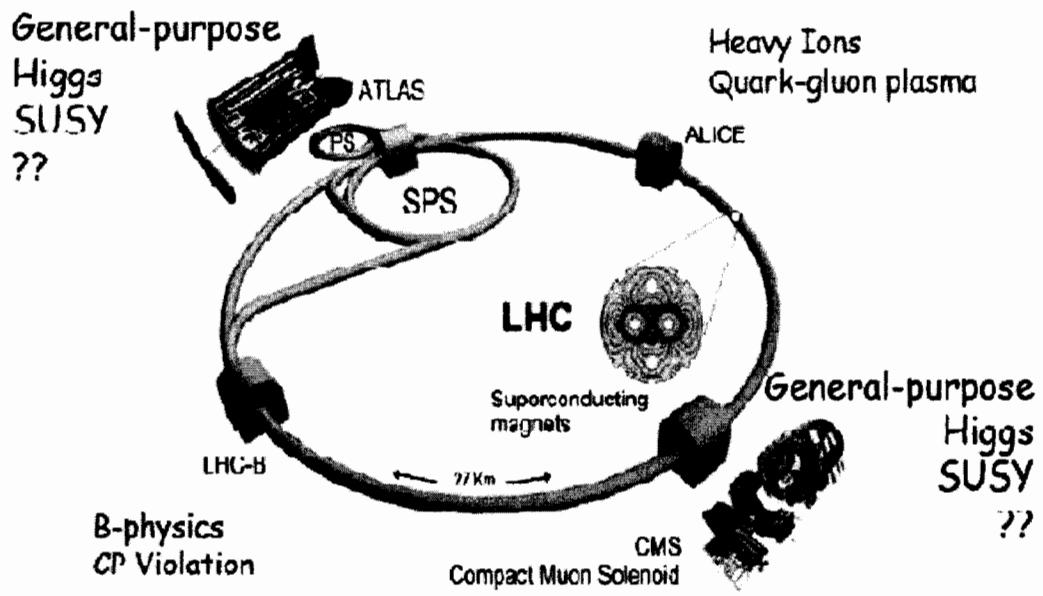

Fig 2.1: LHC detectors structure

2.2 Compact Muon Solenoid (CMS)

The CMS is one of the two bigger multi-purpose detectors built for the Large Hadron Collider at CERN. The CMS detector consists of several sub-detectors measuring energy, momentum, and charge of particles generated in collisions of proton beams having a centre of mass energy of up to 14 TeV.

2.3 Detector Overview

The CMS detector is designed to study proton-proton collisions at 7 TeV energy at LHC. The cylindrical shape (see Fig. 2.2) is determined by the large superconducting coil

generating a solenoid magnetic field of 4 Tesla the strength of the iron yoke. The yoke is divided into six wheels and a group of three endcap discs at each end of the detector. The magnet yoke is instrumented with muon detectors while the tracking system (based on silicon pixel and silicon strip detectors), the electromagnetic calorimeter (ECAL, made

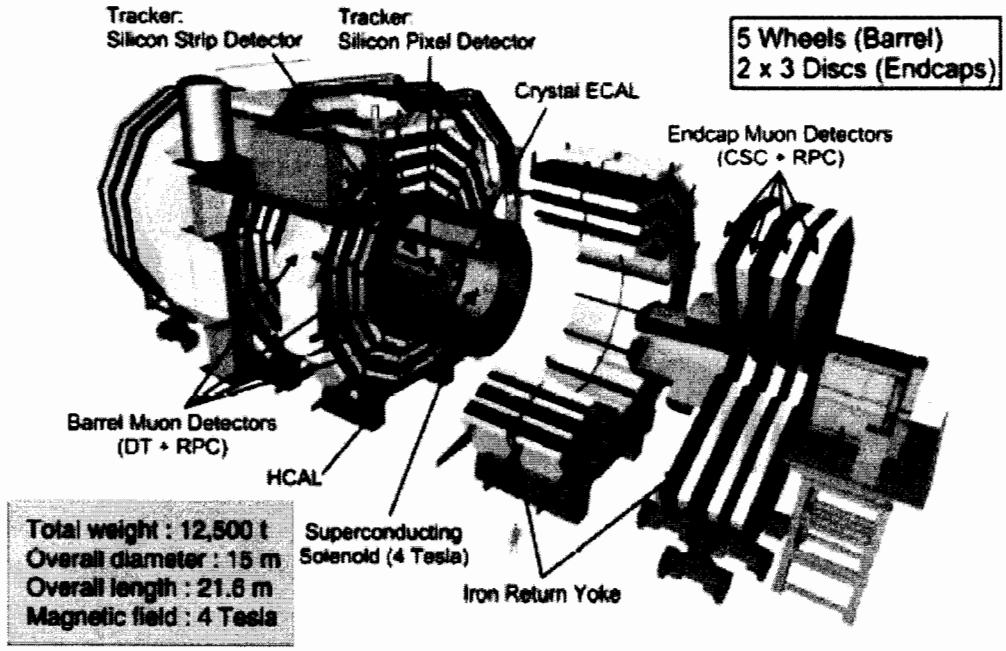

Fig 2.2 Artistic view of CMS detectors

Of $PbWO_4$ crystals) and the hadronic calorimeter (HCAL, made of copper plates interleaved with scintillators) are placed inside the magnet coil [29-33].

2.4 The cosmic ray hodoscope

The structure of the Technion cosmic ray hodoscope is shown in figure 2.3 Groups of 6 to 8 TGC units (12 to 24 wire planes) equipped with front-end electronics are mounted in

the hodoscope as a stack. For each cosmic ray trajectory, the output from each channel of the front-end electronics is read by a TDC (Time to Digital Convertor).

Two arrays of scintillators (2.4 x 1.4 m2) are placed above and below the stack, covering its entire area. The scintillators, equipped with light guides and photo multiplier tubes (PMs) are read out. A coincidence between signals in the two scintillator planes provides a trigger for the cosmic rays.

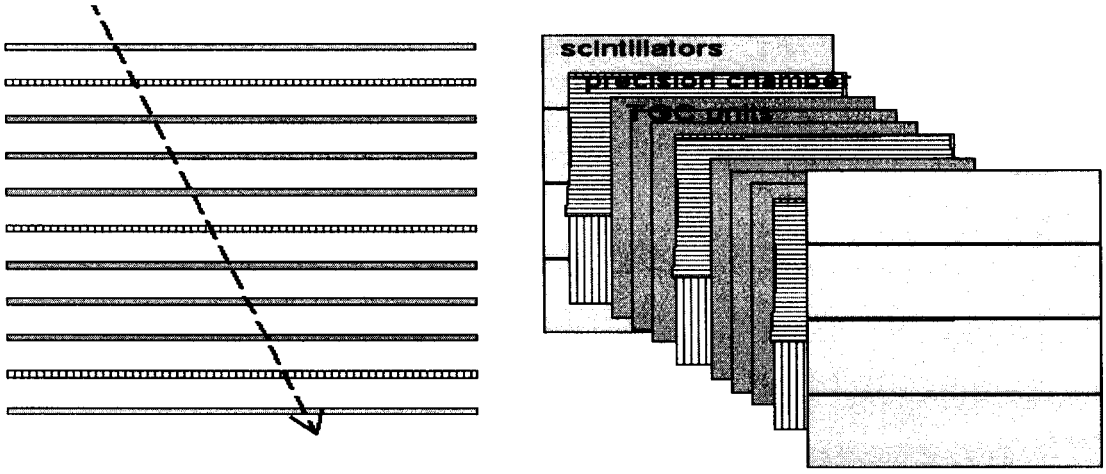

Fig 2-3 The structure of the Technion cosmic ray hodoscope

Precision chambers (2.4 x 1.3 m2 active areas) provide a precise hit position. These precision chambers are specially designed TGCs that have thin strip readout in both x and y. The strip pitch is 3.6 mm resulting in 1024 channels per precision chamber. Along the wires, these chambers allow a determination of hit position to an accuracy of a few microns and the distribution of charge between adjacent strips. The other direction hit is always found at the nearest wires, which gives approximately 1.8 mm precision. The design calls for three such chambers, one between each scintillator plane and the TGC


stack, and the third in the middle of the TGC stack. The hit position in the precision chamber allows the expected hit position in every of the stack TGCs. It will also enable the rejection of muons that had their path deflected by multiple scattering so that their precise position determination is impossible. Currently there are only two precision chambers (top and bottom) in the system. This seems to provide sufficient accuracy to resolve features like the chamber supports. [34]

Another detector DTD (Drift tube chambers) or double-double gaps resistive plate chambers are used in CMS. The Compact Muon Solenoid Barrel resistive plate chambers are high quality tests performed at three different sites, where software and hardware tools are used [35]. This experimental set-up cosmic rays hodoscope is used for quality assurance of the detectors.

Some of the allied work carried out on cosmic ray testing is in Italy. The experimental areas for RPC cosmic ray tests are located in different sites at Italy. Special halls are equipped with cranes, CAEN low and high voltage power supplies, gas-distribution lines using gas racks , online weather stations and data acquisition systems.

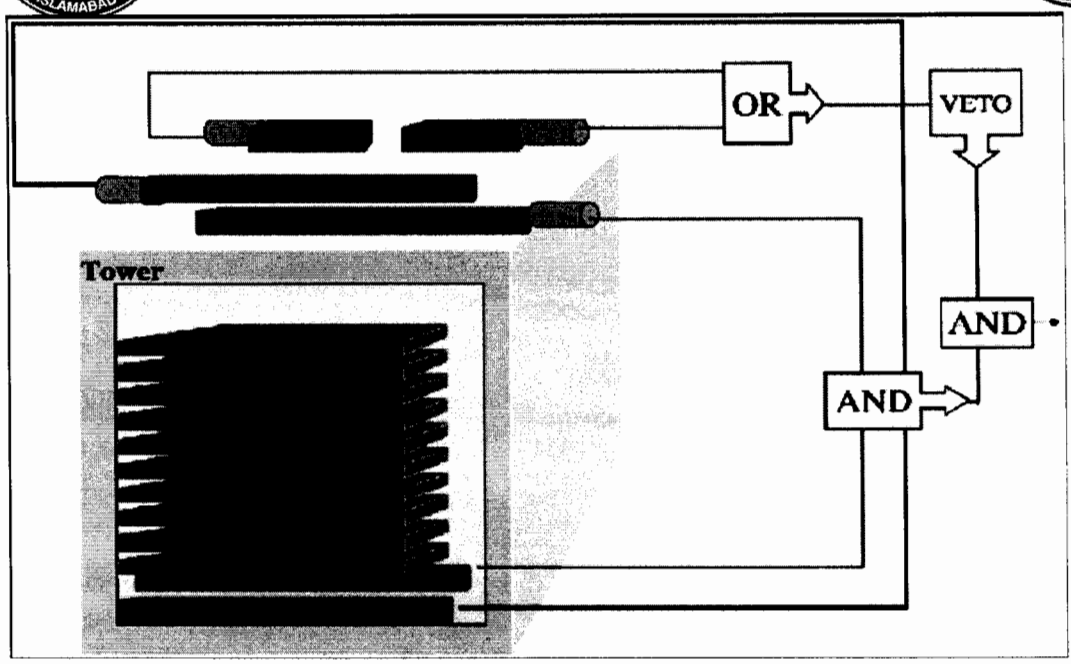

Fig. 2.4 Experimental setup and trigger logic at Pavia (Italy)

The experimental set-up at Pavia Italy is for cosmic ray muon test stand consists of a muon trigger system that is provided by a set of eight or four scintillators located on the top and bottom of the test tower. It is based on two double layers of scintillators covering an area of 125 X 44 cm^2. Fig.2.4 shows the scintillator locations: there are four towers S1, S2 on top and S3, S4 at the bottom of the tower. They are all connected logically (AND) with the mode using coincidence unit. Small 60 X 40 cm^2 plastic scintillators, V1 and V2, which are placed on the top of the tower at a distance of 50 cm from the muon, trigger system. There purposes are to veto electromagnetic showers.

One significant step in the CR (Cosmic Rays) research development is the gradual development of the International Cosmic Ray Service (ICRS) after 1992, including real


time minute and hour data exchange of all CR observatories, allowing the usage of CR data for space weather monitoring and forecasting [37, 38].

Two muon telescopes of cubic design were constructed and are operated in Bulgaria for studying the variations of cosmic rays muon flux. A $1m^2$ telescope is located at Basic Environmental Observatory (BEO) – Moussala – 2925 m above the sea level and is in operation since August 2006. The other muon telescope, with effective area 2.25 m^2, is located at the South- West University – Blagoevgrad – 383 m above sea level. Its data acquisition system was upgraded in November 2007.

Nowadays Nuclear Instrument Modules (NIM) is the main instrument for exploring the Cosmic rays (CR) variations at all CR observatories; they detect the secondary nucleon component of CR and are sensitive to approximately the 0.5 – 20 GeV part of the primary CR spectrum. Along with them, muon telescopes (MT) of different designs are used. The MT are sensitive to a higher range of the primary spectrum (about 10 – 20 GeV and above) and using coincidence techniques alongside, they provide information about the intensities of the CR in different directions. [39]

The data acquisition system for RPC testing has been designed and developed using NIM based trigger and CAMAC electronics for fetching signal from RPC which is available in the laboratory. The hodoscope monitor and RPC data acquisition CAMAC crates are individually controlled by dedicated PC hosts, which the on-line data acquisition system software run. While the hodoscope monitor system collects displays and stores all scalar counter data at equal chosen time intervals continuously, the RPC system waits for the

Cosmic ray muon trigger, to initiate data acquisition for that event. On trigger, the timing (TDC), charge (ADC) and rates (scalars) data are acquired, displayed and stored. Various slow monitor parameters such as temperature, humidity, gas flow into the RPC, applied high voltage, and chambers current etc are also recorded so that we can easily trace various problems with these parameters and calculate result.

2.5 Summary of earlier work on hodoscope

The work is tabulated as below:

S.No	Source	Experimental site	Experimental (purpose of Study)	Detector Types	Tested Parameters	Reference
1.	Cosmic Rays	NASA	charge identification and particle tracking information	Fiber Scintillator	Reject back-scattered particle signals, and to provide a fast shower flag for the TCD trigger without res-orting to the calorimeter system.	29th International Cosmic Ray Conference Pune (2005) 3, 433-436 Design and Tests of the Scintillating Fiber Hodoscopes in the CREAM Instrument
2.	Cosmic rays	INF" Cagliari and University of Cagliari, Italy	study of high-mass muon pairs produced in high energy Pb-Pb interaction with the NA-50 spectrometer at CERN	scintillator counters viewed at both ends by photomultipliers.	study of those signals, accessible in dimuon production, which can be related to the phase transition from ordinary nuclear matter to Quark Gluon Plasma (QGP).	A Scintillator Trigger Hodoscope for the Study of High-Mass Muon Pairs Page 603
3.	Cosmic rays	Status of muon hodoscope URAGAN *Moscow Engineering Physics Institute, Moscow, Russia*	study of heliospheric processes responsible for variations of muon flux at the Earth's surface.	streamer tube chambers	Experimental data from the detectors constitute spatial angular matrices covering the whole celestial hemisphere (at zenith angles from 0± to 80±)	Proceeding of the 31*st* ICRC 2009 Status of muon hodoscope URAGAN
4.	Cosmic Rays	Detectoion of cosmic rays antiproton with heat Pb-bar instruments USA	Study of antiproton flux	Super conductive magnetn, DTD, and Scientillator	Study cosmic rays antiproton with heat Pb-bar with 5 to 50 GeV energy.	Proceeding of the ICRC 2001 Detectoion of cosmic rays antiproton with heat Pb-bar instruments USA page 1691
5.	Cosmic rays	The cosmic ray hodoscope built at the Technion for the test of ATLAS Thin Gap Chambers (TGCs)	The detection of a charged lepton is the primary trigger for many LHC processes	Thin Gap Chambers	Hit position reconstruction	Cosmic rays
6.	Cosmic rays	NCP	Quality assurance of RPC	Scientillator	Cluster size, Strip occupancy, Efficiency, dark current	

Table 2.1: Comparison of various hodoscope facilities existed experimentally and cited in literature.

Chapter 3

Experimental Technique

3.1 Cosmic Rays

Cosmic rays are high energy particles which strike the Earth from outer space. In one second, about 103 cosmic rays strike each square meter area of Earth's atmosphere depends on the sea level height. Cosmic rays are produced in our galaxy by supernova explosions and by-objects such as neutron stars and black holes. Cosmic rays are also produced by the sun during violent events called "coronal mass Ejections" [54]. The cosmic ray air shower is shown in Fig. 3.1.

Cosmic muons, which are produced by decays of different particle in the atmosphere, bombard the earth constantly.

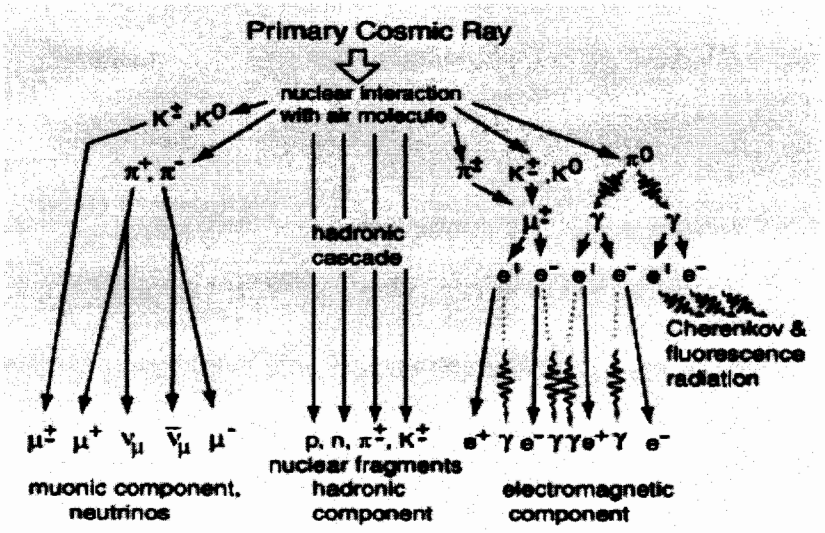

Fig. 3.1 Cosmic ray air shower.

3.1.1 Cosmic Ray Muon Telescope

An arrangement of makeup detector elements like scintillators in space and connected by logic circuitry NIM or TTL such that particle tracks can be identified is termed as "cosmic ray muon telescope". Most often, it is used for triggering purposes. It is based on fast detectors and scintillation counters (used for triggering purpose they very short out put pulse) [42]. A cosmic ray muon telescope is specially prepared for quality assurance of the detectors.

3.1.2 Cosmic Tests

The completed chambers are required for quality control test. These are performed using muons from cosmic rays because cosmic rays are freely available for large detectors. Each chamber is connected with gas and high and low voltage system. High Voltage scans are performed for a number of voltages in the range of 5 – 9.6 kV in steps of 0.5 kV interval.

Each Front-End Board (FEB) can handle 32 channels of a given chamber and connected to the DAQ, thus six cables are needed for each chamber. A Time-to-Digital Converter (TDC) receives input from FEB and transfer the information to the computer.

3.1.3 Cosmic Ray Stand

The completed RPC detectors are put in a cosmic ray stand. The cosmic ray stand is assembled for the systematic investigation of RPCs. This stand is used to check the chamber quality, electronics performance, and overall long term chambers stability. This stand can hold a maximum of ten chambers. There are two rows of scintillators, one at

the top of the stand and one at the bottom, used for triggering purposes. Scintillator detectors are used for triggering.

3.2 Scintillator Counters

Unlike many other particle detectors, which exploit the ionization produced by the passage of a charged particle, scintillator counters rely on the atomic or molecular excitation produced. De-excitation then results in the emission of light, a process known as fluorescence. This light then acts as a detectable signal. However, the material detecting the particle must be transparent to its own signal, which is not naturally the case

There are two main types of scintillators:

1. **Inorganic**, such as sodium iodide (NaI).
2. **Organic**, plastic such as polystyrene or Plexiglas ($C5H8O_2$).

The Inorganic Scintillator is made a special piece of plastic sodium iodide called "scintillator" .When charged particles, such as cosmic rays pass through the NI Scintillator, they excite the atoms in the plastic by giving them some energy. The excited atoms then de-excite by losing this energy and emitting some photons of light. The light is detected by a equipment called a "photomultiplier" (PMT). The photomultiplier, as its name suggests, multiplies the small flash of light into a large electrical signal that can be measured. From the size of the electronic signal we can tell how many particles passes through the scintillator. The Scintillator may have an area of a few cm^2, depending on the

application. A simple Scintillator counter is shown in Fig. 3.2. Light travels along the thin sheet undergoing many total internal reflections. Most light travels close to the critical angle, and the surfaces must

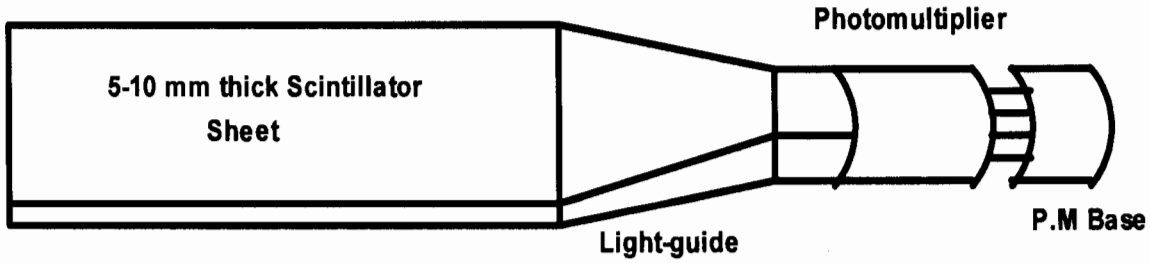

Fig. 3.2 Simple Scintillator counters with PMT.

be highly polished to avoid losses. The light is converted to an electrical signal and amplified by a photomultiplier [43]. A light guide, couples the Scintillator to the photomultiplier tube. Light entering from its one end, "guided" by internally reflecting it back and forth between the interior walls and is focused on other end. For a simple counter, this may be in the shape of a "fish tail", but more contorted shapes may be adopted, e.g. to couple many Scintillator sheets to the same photomultiplier.

3.2.1 Working of Scintillator Counters

Scintillator counters can detect the charge particle from cosmic rays for testing of the different type of detectors. Two planes of counters reveal which hits to the chambers are cosmic muons. Using this system tracking of cosmic muons become easy. The top rack of the counters will interact with anything that goes through it. If the particle gets to the

bottom rack of counters, then that particle is most likely a muon. If the particle does not hit the bottom rack, then it is a soft component that interacted with the Scintillator [44].

3.3 Photomultiplier Tube (PMT)

The main components of a PMT is shown in Fig. 3.3. A photon passes the PMT window, it strikes the photocathode, which responds by emitting electrons. These electrons pass to the first dynode, then to the second, then to the third, and so on to the anode, due to the steadily decreasing electric potentials placed on the dynodes by the divider.

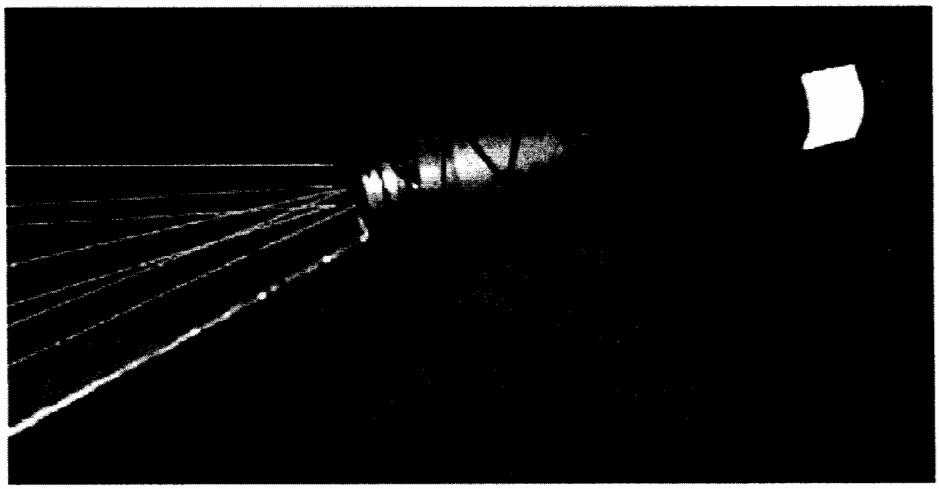

Fig. 3.3 Diagram of how a PMT works:?

Furthermore, when one electron hits a dynode, several more electrons are emitted. An avalanche occurs as the number of electrons increases exponentially. In this way, the Scintillator and PMTs convert incident cosmic rays into an electrical signal. The PMT is vital to this operation since it enhances the signal by a series of electron avalanches that will eventually form a current. The computers will read this current from the top and

bottom rack of scintillators to determine if the particle is indeed a muon. The scintillator counters allows the muon chambers to be assessed for proper function.

However, noise in the PMT and the plastic in the Scintillator emits light spontaneously that can interfere with particle detection. As the applied voltage increases, the multiplier amplifies the small random noise in the electronics of the PMT along with the electrons caused by light from the scintillator. This amplified noise overshadows much of the signal from the scintillator. Furthermore, light from the Scintillator is not always a result of incident charged particles. This light also enters the PMTs and mingled with the signal.

3.3.1 Properties of Scintillator Counters

The most important properties of Scintillator counters are:

- Fast time response: light generated almost immediately after particle passes through the Scintillator, photo detectors give fast electrical signal.
- Using pulse height: it can count number of particles. The larger the signal size, the greater the number of particles.
- Position information: Based on size of active Scintillator.

  Scintillator counters are continuously sensitive and have a fast response, they provide ideal trigger for other detectors.

3.3.2 The development of Scintillator detector

We have built and test your own Scintillator detector in the lab at NCP, Islamabad. Some operational steps are described below:

1. Wrap the plastic Scintillator with aluminum reflecting tape to maximize the light output from one end of light guided media of the Scintillator.

2. Wrap the plastic Scintillator with black tape to protect entering the external light.

3. Attach the Scintillator to the photomultiplier tube using coupling optical grease (used for optical contact) and fix it with more black tape at the base.

4. Mount the photomultiplier tube with one end of the plastic scintillators.

5. Connect the high voltage and look at the pulses from Scintillator detector with the help of oscilloscope.

6. Connect the output of Scintillator to the first NIM module (Discriminator).

3.3.3 Scintillator arrangement for Muon Telescope

There are 18 scintillators required for RPC testing; 8 of them are placed on top of RPCs, 8 on bottom to cover whole area of RPC and two work as acceptance counters. All these counters were obtained from old DELPHI experiment and were made in Russia. These are made of an organic material "polystirol" with scintillation compound. The original dimensions of the scintillators are 350 cm × 20 cm × 1 cm. These scintillators are cut to the required dimensions (according to the dimensions of RPCs) and then polished. Now the counters have dimensions of 190 cm × 20 cm × 1 cm. The area formed by these counters in top and bottom layers of muon telescope is 190 cm × 160 cm. Then the light insulation is applied to avoid background counts and to get good efficiency of the scintillators. Steps for light insulation are:

- Clean the Scintillator counters using alcohol.

- A Mylar sheet of < 50 microns of Aluminum foil is placed on the scintillator.
- A layer of photo-paper of > 100 microns is then taped over it.
- Multi layers tape is pasted to avoid damaging light insulation and Scintillator.

After light insulation, the most important step is to attach PMT with Scintillator. The ends of the scintillators were heated, compressed and then attached to the PMT by using optical gel. The PMTs have multi-alkaline photo-cathode (FEU-118) with eleven dynodes. The area of sensitivity of this PMT is 46 mm in diameter. The complete unit is placed in housing.

3.3.4 Operating Voltage

Operating voltage of the PMT is very critical to determine a good output from it and to avoid its damage. Therefore, to find the operating voltage, coincidence technique is used.

The steps followed are:

- Fixing the threshold of both counters
- Fixing the voltage of both counters at 1200 V
- Making coincidence of both counters
- Reducing voltage of one counter to 1000 V, keeping the other at 1200 V
- Initialize the setup to increase the voltage of this counter till a certain saturation in counts is not achieved
- The saturation in counts is the operating voltage of second Scintillator

This way, the operating voltage of these scintillators lie between 1250 V to 1800 V.

3.5 Trigger Setup Modules

The following modules are used for trigger generation:

1. Power Supply SY1527 – Universal multi-channel with A1733N module
2. Coincidence Unit – Quard Coincidence
3. Discriminator – Octal discriminator Model
4. Oscilloscope – Tektronics, 500 MHz

3.5.1 Power Supply SY1527

A High Voltage power supply is required for the operation of RPCs and scintillator counters, which can provide sophisticated and wide range of varying voltages and currents. For scintillator operation we need a power supply with range of 1.0 – 1.4 kV and to power up RPCs we need a power supply with maximum range of 10 kV.

The High Voltage power supply distribution is based on the Universal Multi-channel CAEN-SY1527 unit which has internal processor and network connections. Dedicated software run with Graphical User Interface (GUI) is stored in built and selectively records the values to monitor the high voltage channels. Each chamber is supplied by two HV channels, as shown in Fig. 3-4. One High Voltage channel supplies voltage to the top cut gaps and other to the bottom full gap.

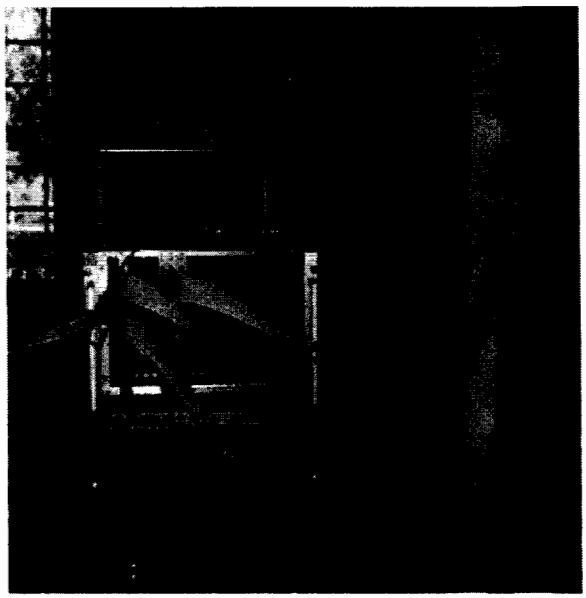

Fig 3.4 CAEN Power Supply (Our Developed System at NCP)

On the display of Power Supply, there are many columns, but few of them are of our prime interest. The first column shows the number of chambers and scintillators, which are going to be tested. Second column shows the input voltage, which we give to the chambers and to the scintillators.

During the testing process, the voltage of the scintillators is fixed whereas the voltage of the chambers is varied as mentioned in the testing procedure. Third column shows the current which we fix for the chambers and the scintillators. We fix this current as a threshold and whenever the current increases from this threshold value, the chamber and/or the scintillator is automatically switched off. Fourth shows as to how much current is flowing through the chambers and the scintillators. Whenever the current increases the threshold value, the next column shows OVC (over current flow) relative to that chamber and/or the scintillator.

3.5.2 Signal Cables

• All input channels are terminated to match a 50 Ω signal cables or terminators. One end of signal cable is connected with scintillator and other with NIM module.

• We use 32 LEMO connectors on the scintillators and 20 LEMO connectors on the NIM modules.

• We use 32 High Voltage power cables to power up the scintillators. They can operate below 5 kV with the current of 1 A. If the voltage increase up to 5 kV, it can cause the damage to the cables. We operate the scintillators between 1.2 – 1.6 kV.

• 50 Ω data/ribbon cables are used to take data from RPCs to TDCs. We use connectors for these cables.

• We use 20 High Voltage power cables to power up the 10 RPCs. One for cut gap and one for full gap. They can operate below 15 kV with the current of 1 A. If the voltage increases up to 15 kV, it can cause the damage of the cables. We operate the RPCs between 8.0–9.6 kV.

• Length of each signal cable, power cable for scintillator, data/ribbon cable, power cable for RPCs is 20 ft approximately.

• All connectors used in cosmic ray muon telescope setup are made in the HEP lab, at NCP Islamabad.

3.5.3 Discriminator

The CAEN NIM model N840 is an 8 channel leading edge discriminator housed in a single width NIM module. The module accepts eight negative inputs and produce eight NIM output on front end panel LEMO 00 connectors.

The discriminator produces an output pulse whose width is adjustable in a range from 5 ns to 40 ns. Each channel can work both in Updating and Non-Updating mode according to on-board jumper's setting. The discriminator thresholds are settable in a range from -1 mV to -255 mV with 1 mV step, with an 8-bit Digital to Analog Converter.

The back panel houses VETO and TEST inputs and logical OR output and the Current Sum (Σ) Output, which generates a current proportional to the input multiplicity, A four digit LED display provides information on the module's status on front of the module.

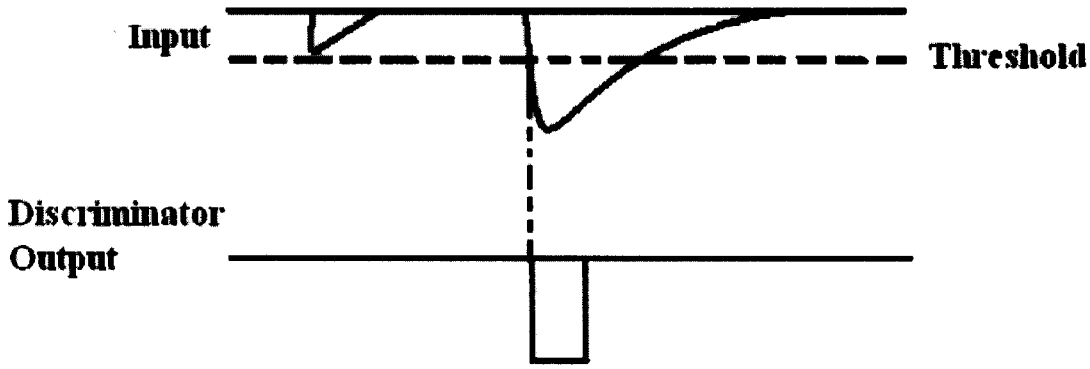

Fig. 3.5: Discriminator operation: only signals whose amplitude is greater than the fixed Thresholds trigger an output signal.

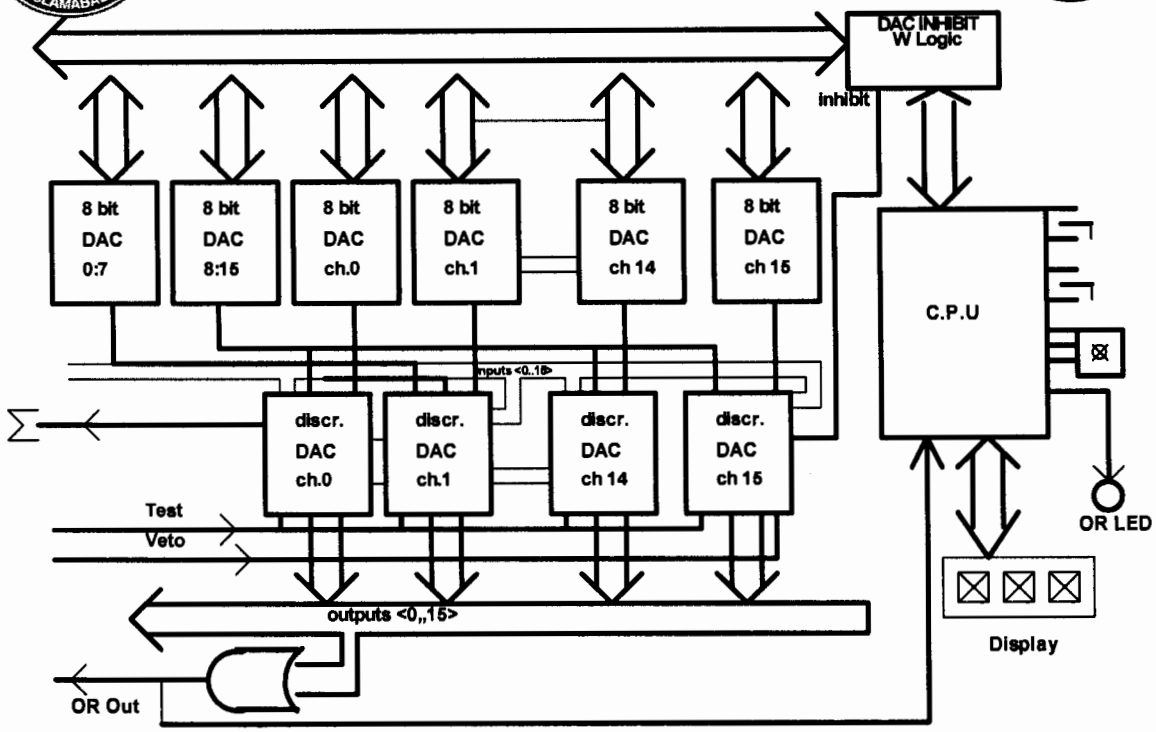

Fig. 3.6: Functional Diagram of Discriminator.

3.5.4 Coincidence Unit

The coincidence unit determines if two or more logic signals are coincident in time and generates a logic signal if true and no signal if false. The electronic digital pulse of a coincidence between two pulses may be made in a number of ways [48]. Simple method used here is to sum the two input pulses and to pass the summed pulse through a discriminator set at a height just below the sum of two logic pulses. This method is shown in Fig.. Obviously, the sum pulse will only be great enough to trigger the discriminator when the input pulses are sufficiently close in time to overlap. The definition of coincidence, here, actually means coincident within a time such that the pulses overlap. This time period determines the resolving time of the coincidence and

depends on the widths of the signals and the minimum overlap required by the electronics.

The coincidence unit is one example of a more general class of units known as the logic gate. These are units which perform the equivalent of Boolean logic operation on the input signals. The coincidence unit, for example, essentially, performs the logical "AND" operation on the pulses.

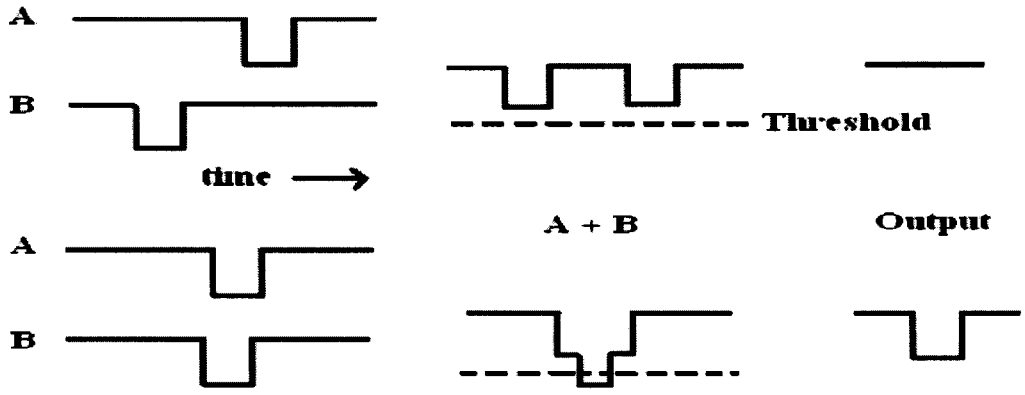

Fig. 3.7 Output of coincidence unit

The summing method for determining the coincidence of two signals is shown in Fig. 3.3. The pulses are first summed and then sent through a discriminator set at a level just below twice the logic signal amplitude.

3.5.5 Efficiency of Scintillator Counters

The efficiency of scintillators is also an important parameter for the quality assurance of our project. For their good performance, it is necessary to determine their efficiency. The logic of the same is shown in Fig. 3.8

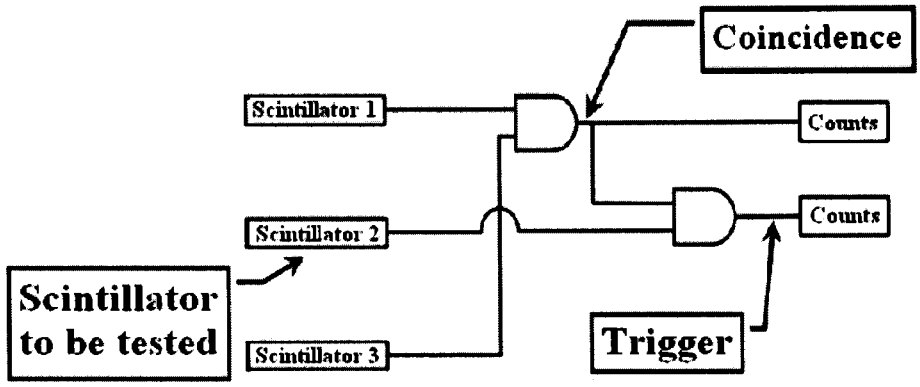

Fig 3.8: Logic for Efficiency Measurement

Two scintillators, Scintillator 1 and 3 are placed in coincidence and their counts are collected. These are called coincidence counts. Then a Scintillator 2, which is to be tested for its efficiency is placed in between these two scintillators and a trigger is made with the coincidence and Scintillator 2. Counts with Scintillator 2 are called trigger counts. The efficiency of these Scintillators is calculated by using this equation:

$$\eta\,(\%) = \frac{\text{Trigger}}{\text{Coincidence}} \times 100 \qquad \text{----------Eq.3.5.6}$$

Using this technique efficiency of all 18 scintillators is determined. A characteristics efficiency plot is shown in the Fig. 3.5. Power supply used for these efficiency measurements is Universal Multi-channel CAEN SY1527 power supply with A1733 module.

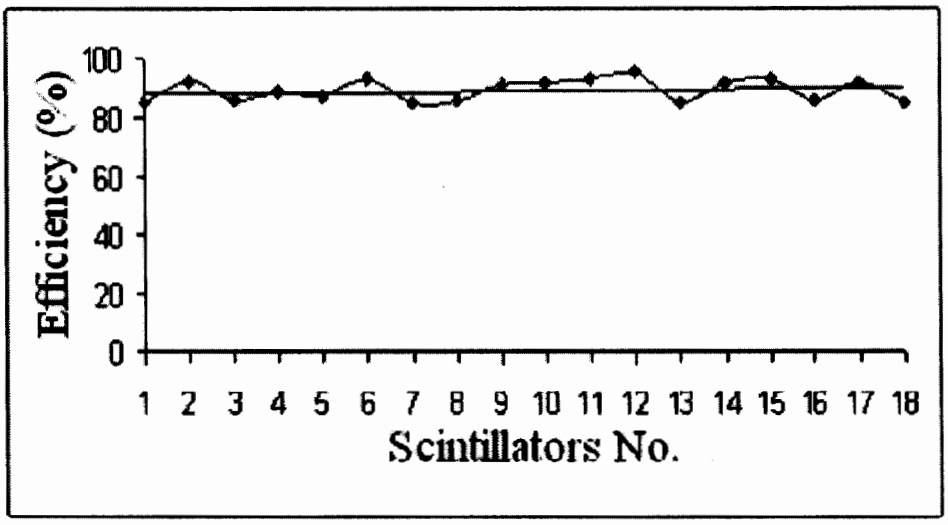

Fig. 3.9 A Characteristic Efficiency Plot (Original Data)

3.6 Resistive Plate Chamber RPC

RPCs have an excellent time resolution as compared with the scintillators, and requisite spatial resolution. Their main purpose is to provide information to the level-1 trigger. The RPC contains two layers of gas gaps with a sheet of copper readout strips sandwiched between them, as shown in Fig. 3.6. Gas gaps are made of two thin sheets of high resistivity bakelite which act as the electrodes. Within the RPC, the electric field is uniform. Exponential multiplication of the electrons release by the ionizing particles in the gas gaps gives the signal amplification on to the strip. The cumulative effect of avalanches gives the detected signal, which is collected by the readout strips.

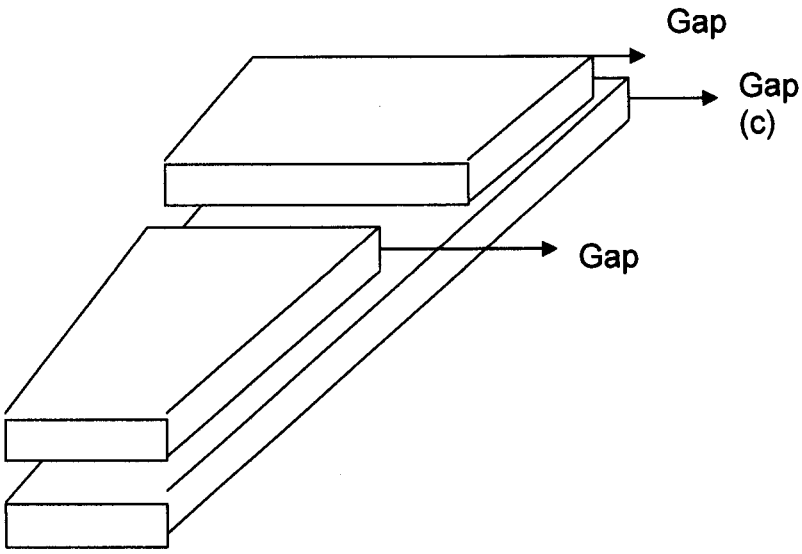

Fig: 3.10 RPC construction with Top and Bottom Gaps

The use of thin Bakelite sheets allows for the construction of large and thin chambers, capable of operating at a high rate and gas gain without the development of sparks. The rate capability of RPC can reach several thousand Hz/cm^2, depending on the selection of resistivity and plate thickness of the gas gaps. The thin gap and high gain of an RPC makes it possible to precisely measure the small delay for the ionizing particle such as a muon. The delay of pulse, the resolution, and the efficiency of chamber are largely determined by the threshold setting of the chamber. The selection of an appropriate threshold setting allows for the detection of a signal dominated by electrons generated near the cathode. A measure of the muon's momentum can be obtained by tracking the strip hits in conjunction with other inner detectors in CMS.

3.6.1 Front-End Board (FEB)

The RPC FEBs handle 32 channels. Each FEB contains four Front-End Chips (FEC). The FEC is an 8-channel ASIC, consisting of amplifier, discriminator, mono-stable and differential line driver.

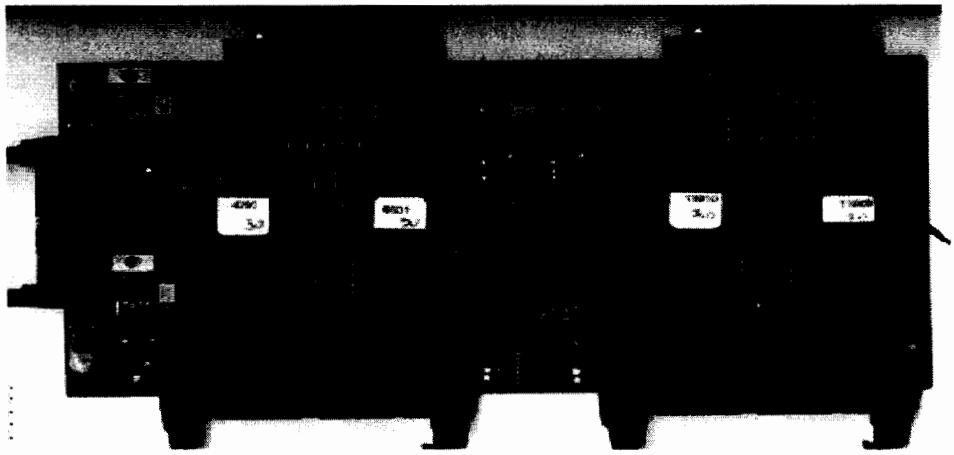

Fig. 3.11 Front-End Board

The RPC readout strips are connected to FEBs by co-axial cables terminated by the adaptor boards, whose shapes are optimized to obtain the right channel characteristic impedance and to have the same arrival time for all channels on the FEB input. To simplify things we have decided to keep the same number of strips for each FEB belonging to the same layer, requiring this number is less than or equal to 32. This is obtained provided that the FEB has a minimum width. The implemented FEB has a size of $110.6 \times 228.6\ mm^2$.

The RPC parameters to be controlled consist of RPC Detector Control (RPC-DC). This includes HV and LV control for the chamber and FEB, setting and checking of discriminator thresholds on the FEB, and temperature and pressure control. This group of parameters will be controlled directly on the FEB.

3.6.2 FEB Functional Description

The purpose of FEB is to house the electronics that produce the signal for high level processing. The input (information from the RPC) is processed and delivered to the trigger system by FEBs. Each RPC consists of 3 FEBs. The FEB is directly connected to the RPC and contains 32 channels of RPC front-end electronics. Each FEB device has four test inputs, one for every two readout channels. For simplicity, however, we intend to use only one test input per two channels, connecting 2 test inputs together at board level. The test inputs will be check the channel connectivity with the detectors and to monitor dead channels. Additionally, they establish the delay between the FEB and Link Board and so to use the right clock phase for synchronization. The threshold input will fix the equivalent charge threshold value applied to the discriminator, ranging between 10 fC and a maximum of 300 fC.

3.6.3 VME Crate Controller & Data Registration

There are different types of modules connected in the VME crate. We have different types of input data to the modules of the crate. These inputs come from RPCs and muon telescope. Each and every module of the crate has its own function to handle these inputs.

VME crate controller which handles all modules, and is connected through a MXI — 2 cable and PCI card with the computer.

We have information of all the modules connected in crate controller, and also data registers in which data (coming from the detector(s) and hodoscope) is stored temporarily. We have a task to get this (hexadecimal format) data from these registers and store it permanently on a computer. For this purpose, we have windows based software for the PCI card which is configured well and working properly. But we have to switch the operating system to LINUX. For this purpose we have already got LINUX based software for the same PCI card which is also configured.

3.6.4 Time-to-Digital Converter

Inputs and Outputs

The module has two frontal NIM inputs for the clock and trigger. These 2 signals are distributed by the Master module on ECL levels to the crate backplane, if the crate is properly terminated on the connector JP3.

Clock

The module needs a clock signal not faster than 50 MHz. Inside the module there is a PLL that duplicates the clock frequency in order to catch up the maximum temporal resolution of 10 ns. The clock of the module can be taken from the frontal NIM input, from the backplane of the crate either in ECL logic or generated internally from a quartz oscillator running at 50 MHz.


Trigger

The module uses this signal to stop the acquisition (Common Stop). It is sampled at the frequency (max. 100 MHz), so its width should be at least 10 ns. The acquisition is stopped on its rising edge.

The module can receive the trigger from the NIM input (Jumper TRIGGER set on EXT) or from the backplane (Jumper TRIGGER set on INT).

Inputs

The board accepts up to 64 LVDS inputs. The signals are sampled at the clock frequency (max.100 MHz) so their width should be at least 10 ns.

3.6.5 Detection of Muons

When charged particles (mostly muons) ionize the gas of the RPC, an avalanche is formed by multiplication in the gas particle or ions [49]. The avalanche charge is collected by the anode and produces an induced charge on the external readout strips, representing the prompt signal of the RPC. The readout strips are connected to the FEBs by co-axial cables via the adaptor boards. The FEBs are connected with TDCs through connectors which are put in VME crate. A TDC is used for read out the information from the FEBs and transfer the information to the computer. Signals from RPC is amplified and digitalized and convert into LVDS in the FEB. The LVDS signals are fed into the START inputs of the multi-hit TDC and the trigger signals from scintillators (discriminator) into the STOP inputs of the TDC. Signals from chamber are also fed into the common STOP inputs of the TDCs. When a DAQ detected trigger signal the data

from the TDC and stores it in a binary output file by using PCI NI-MXI-2 modules for further offline analysis. In parallel the program continuously shows the plots which enables to monitor the quality of the data online and the equipment performances. The plots are automatically stored in the Data Base.

3.6.6 Resistive Plate Chamber Efficiency:

Detectors efficiency is obtained with the "coincidence" method by evaluating the ratio between the number of events received by the RPC (least one fired strip in the trigger window 40 ns) and the total number of recorded events, with correction for spurious hits [50].

The efficiency is defined as:

$$\varepsilon = \frac{[(Nob/Nt) - Ps]}{1 - Ps} \times 100 \qquad \textbf{Eq : 3}$$

Where N_{ob} is defined as the number of observed events. N_t is defined as the number of total events. and P_s is defined as the probability of the spurious hits. The probability of the spurious hits is determined by counting the hits in a time window delayed 40 ns after the trigger. The value of the efficiency should be greater than 95% at operating voltages and the efficiency plateau starts at 9.5 kV. For good performances of RPC, its efficiency plateau should lie in the range of 300 V. The maximum efficiency and length of plateau depends upon the gas mixture. The efficiency plots of the chambers CMS-RE-2/2-PK-032 and CMS-RE-2/3-PK-015 are shown in Fig. 3.12.

When the voltage is small, the ionization in the chamber is small which results in small current in the gap. As we increase the voltage, efficiency also increases, which shows that the ionization in the gap is large and chamber draws large current. After 9.2 kV the behavior of the efficiency is approximately linear. The operating voltage starts at 9.2 kV to 9.6 kV and operating plateau is greater than 300 volts. The value of efficiency is almost > 95% at high voltage.

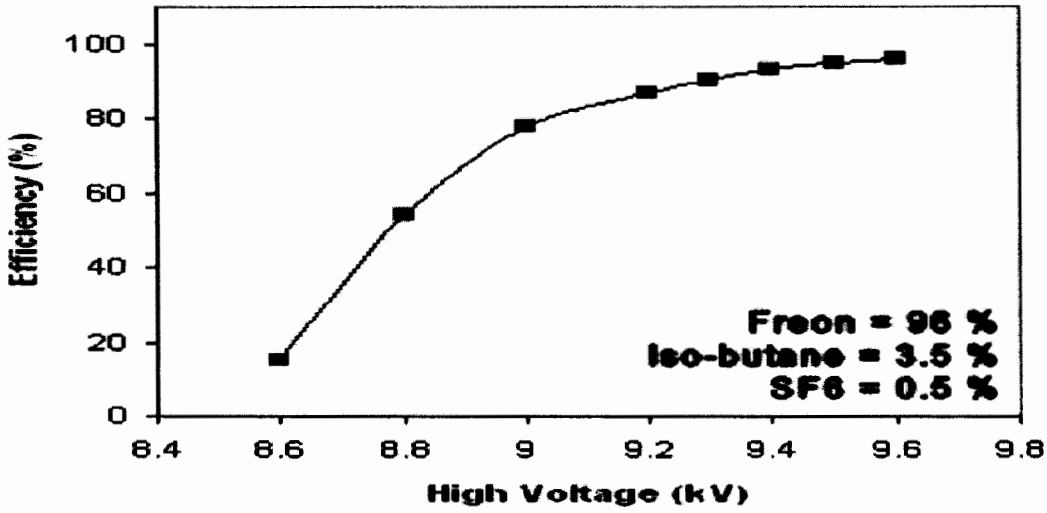

Fig.3.12 Efficiency of RPC (original data taken from NCP)

3.6.7 Dark Current

For entire period the chamber is connected to high voltage currents through each of the gas gaps. Given that current should be constant in time, any major deviations from this are indicators of a problem with the gas gaps or chamber electronics. For the efficient performance of the chamber, the value of the dark current should be minimum. Temperature and humidity in the lab is also recorded because the performance of RPCs

and resistivity of bakelite are functions of these parameters. Plots of dark current for the chamber CMS-RE-2/3-PK-015 are shown in Fig. 3-13 .

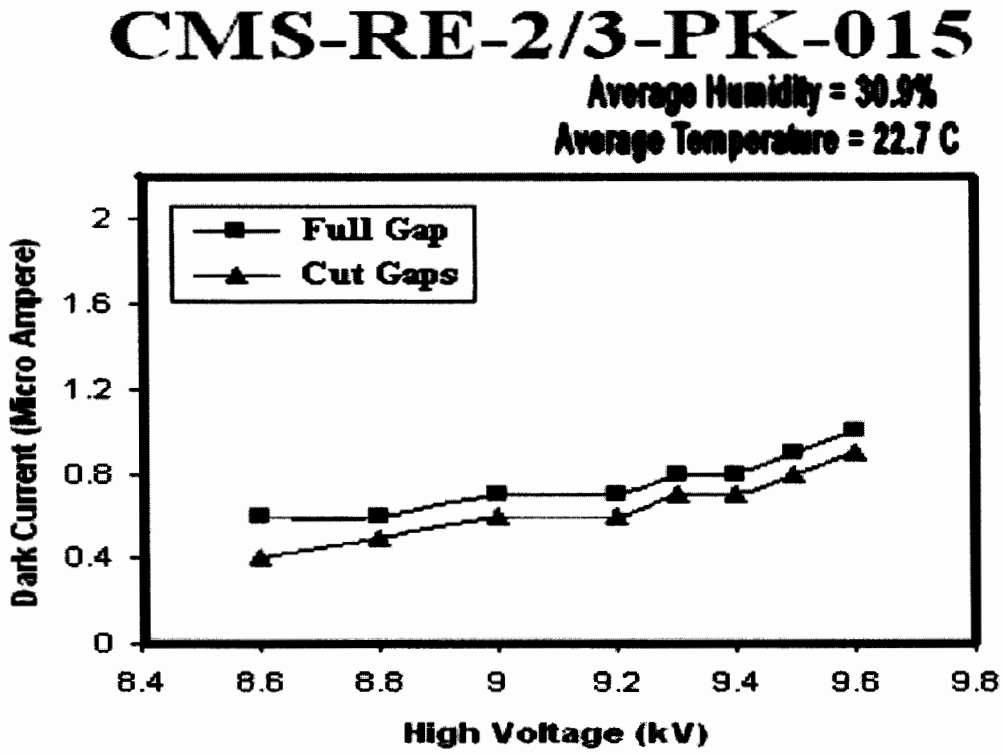

Fig 3.13: Plot of dark current for CMS-RE-2/3-PK-015

In these plots the dark current is less than 5 μA, which is the requirement of CMS. Finally all above parameters are analyzed, from which the overall behavior of the chamber is reflected, and in this way good RPCs are distinguished.

3.6.8 Gas System for RPC Testing

For high voltage tests, the RPCs are placed in the cosmic ray stand and gas gaps are filled with gas, which contains a mixture of Freon (C2H2F4) 97%, Isobutane (C4H10) 2.5% and Sulphur hexafluoride (SF6) 0.5%. The addition of SF6, allowed reducing the streamer charge and extending the counting rate capability. In this section we are mainly concerned with the gas system of the RPCs. The gas system is shown in Fig. 3.14

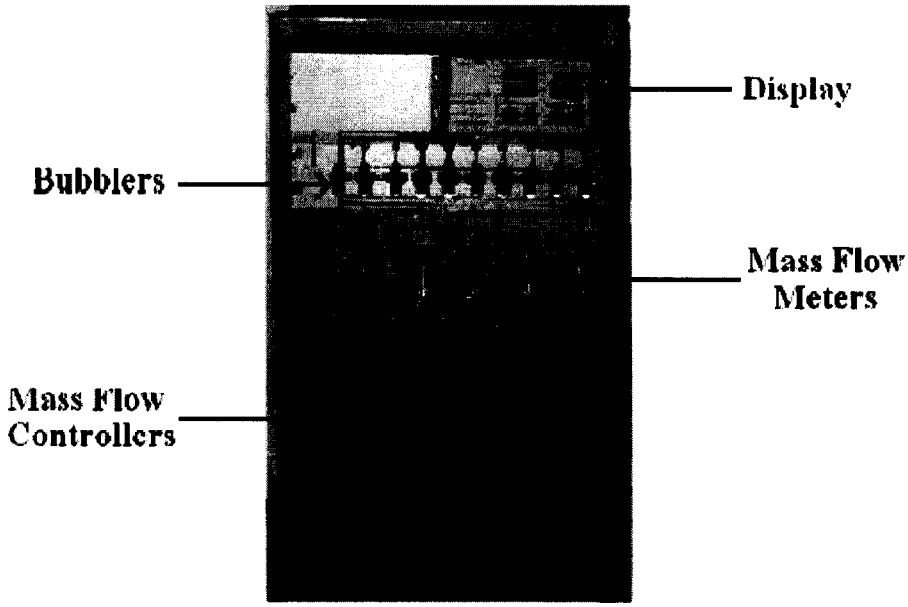

Fig: 3.14 Gas Distribution system

3.6.9 Gas Requirement for RPCs:

The dimensions of the RPC are shown in Fig. 2-10. All endcap RPCs are trapezoidal in shape, the values of the dimensions are given in Table 3.1. The naming scheme for the chamber representation is as follows:

RE n/m, n = Station Number, m = Region number

No. of gas gaps = 3

Width of the gap = 2 mm

Let's take $RE_{2/2}$ and RE 3/2 chambers as an illustration. These two types of RPCs have same dimensions therefore their gas requirements are same.

Area of the RPCs is given in the Table 3.1

Total volume of RPC = no. of gaps × width of each gap × area of RPC

(For this volume total gas required is = 5.6 liters)

We are using three gases: Freon, Isobutane and SF6 whose percentages are 97, 2.5 and 0.5, respectively.

Table3.1 Dimensions of RPC

Station	A (mm)	B (mm)	C (mm)	D (mm)	Area (m^2)
RE 2/2, RE 3/2	1693	979	684	1687	1.403
RE 2/3, RE 3/3	1961	1323	981	1954	1.917

From the mass flow meters the maximum flow rate of each gas may be determined. So percentage of each gas on the power supply display will be:

Percentage of Freon = 14.7%

Percentage of Isobutene = 12.6%

Percentage of SF6 = 10.5%

3.7 Working of the Gas System

Gas comes from the cylinders through pipes into the mass flow meters, which are calibrated for each gas (Freon, Isobutene, and SF6). Mass flow meters monitor the flow rate of each gas according to the requirement of the RPCs. There are six inputs and four outputs channels in the power supply. The gases enter into the big cylinder where all gases mix up according to the required percentage mentioned. After that, gases enter into two cylinders which are connected through "U" shaped pipe, here mixture is controlled from the front of the gas system for each RPC through mixture controllers. Then gases enter into the cycling system through bubblers. From bubblers we can not only see the flow of the gas, but also observe the leakage of the gas from the RPCs. There is exhaust through which all the undesired gases, which are formed after reacting the three gases goes outside the system and remaining gases enter the cycling process again.

3.8 Data Acquisition System

The Data Acquisition System (DAQ) itself is a major field and it is extensively used in many disciplines with different requirements. A DAQ system consists of seven elements as shown in Fig. 3-15 and they are same in every system, which is used for the data acquisition purpose.

The elements we expect to see in a DAQ System are sensors, data transmission links, a collecting means (such as data acquisition board), a processor, a clock, triggering and/or control hardware and a means of laying down a permanent electronic record.

3.8.1 Parts of DAQ System

A DAQ system equipped with enormous and latest technology of electronics, which meet the different criteria of an experiment are specially designed according to the requirement of an experiment. When all the parts of a DAQ system are combined, then the system is ready to perform the specific applications. Maximum electronics used, in LHC experiment, is based on VME standards. There are three major parts on which a DAQ system comprises, which are:

- **CAMAC** (Computer Automated Measurement and Control)
- **VME** (Versa Module Euro-card)
- **NIM** (Nuclear Instrument Module)

These are three different parts, which are used in many different experiments for data acquisition. They are further divided into many other modules like Time-to-Digital Converter (TDC), scalers, discriminators, amplifiers and many other peripheral devices.

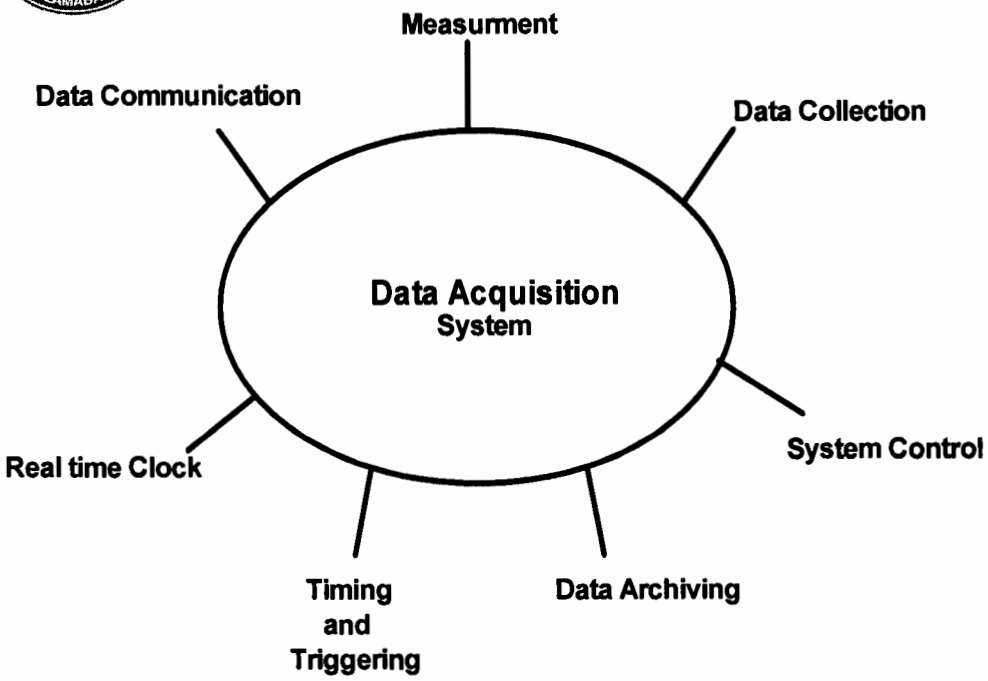

Fig. 3.15 Parts of DAQ system

3.8.2 Installation of DAQ software

Before starting off a DAQ program, we need to prepare DAQ machine. DAQ have some requirements and procedure. These requirement and procedure are as follows:

- Installation Procedure

- Install Linux Red Hat 7.3 using CERN specified installation method.
- Install gcc 3.2.3
- Create a partition labeled "/data".
- Insert NI MXI-2 PCI Card into the machine.
- Insert CD of VISA libraries into the CDROM & run INSTALL script to install VISA libraries by selecting default options.


- Insert NI MXI-2 Card Driver Disk into the CDROM & change the directory to LINUX & run INSTALL script by selecting default options.
- Include driver initialization script path /usr/local/nivxi/sys/load_vxi into the file /etc/rc.local .
- Installation of ROOT
    - Login as the root user
    - Untar ROOT distribution
    - cd root
    - ./configure –prefix = /usr/local
    - gmake
    - gmake cintdlls
    - gmake install
- Installation of DAQ
    - Create a user daq
    - cd CAENHVWrapper_2_11
    - make
    - make install
    - untar daq distribution
    - cd daq-1.0.0-pak
    - ./clean_all.csh
    - ./Build.csh
    - mkdir /var/log/daqrpc
    - Copy all the configuration files to this directory.
    - Change ownership of this directory to daq
- Set library paths
    - Perform su - root
    - Include the path /usr/local/lib/root in /etc/ld.so.conf
    - Include the path daq-1.0.0-pak/lib to /etc/ld.so.conf
    - Run the command ldconfig –v
- Set hardware addresses for all the Time to Digital Converters (TDCs) & IO register.
- Verify the hardware addresses using NIvisaic utility.

Now we are ready to take cosmic run using DAQ system.

3.8.3 Cosmic Ray efficiency test using DAQ

RPC detectors that pass the visual inspection tests are moved to the Cosmic Rays efficiency test bench hodoscope. The scope of the efficiency test is to measure the time response and the efficiency of the Trigger Gate Counters. An online DAQ program, running on the VME crate based on Pentium CPU, is controlling the test. Every DAQ run begins with readout of 10,000/20,000 events with software generated sequential trigger. When a trigger is detected the DAQ reads the data from the TDC, the Analog to digital converter and the High Voltage controller, and stores all of it in a binary output file for further offline analysis.

A good chamber has at least 95% efficiency of its active area. The time response is less than 25 ns or 40 MHz. A C++ and JAVA offline analysis program reads the binary output file of the DAQ code and processes it for generating plots. The offline program first reads the threshold parameters of the TDC channels. Then its sequentially reads the information stored for each muon bunching crossing [41].

We have also developed DAQ on-line software that will measure RPCs efficiency, cluster size, strip occupancy using JAVA.

DAQ online was a tool developed using java [19] and web services technology [20]. The main feature of DAQ online was to provide the user a facility to process data and create plots by sending requests to remote servers. Since DAQ online was based on web services technology, it is very easy to do distributed data processing. Data received from


an RPC is then converted into "xml" format using an "xml" conversion tool which was provided with in the developed system.

3.8.4 Online Data Acquisition

These "xml" files are stored on one of many servers. Users can connect to any of the servers and process the data. DAQ online also provides a caching facility of a particular "run number" so next time the user do not have to go through the network to view or create plots for a given run number which was already been processed in the past. This facility is very useful when we had a limited network bandwidth or unstable network resources.

3.9 JAVA

The characteristic of JAVA is port-ability, which means that program is platform independent and computer program written in the java language must run similarly on any supported hardware/operating system. The JAVA runtime software environment provides the libraries, the java virtual Machine, and other components to run applets and application written in the java programming language. We are using JAVA for remotely connected front-end with web services.

3.10 Web Services

Web services provide the environment that a programs on one computer talks to each other. One is the server waiting for requests, and the other's the client it needs something done that the server does. The client and the server may talk to each other in a many ways like sockets, pipes and text files, etc.

The server and the client do not have to be on the same machine. One can have an Apache running on some web server machine, and Fire-fox running on a local machine. The client and the server talk to each other in case of Fire-fox and Apache using HTTP

on top of TCP. Apache Axis is an implementation of the Simple Object Access Protocol,(SOAP).

Chapter 4

Result and Discussion

4.1 Introduction to result and Dimension

The main parameters of the RPC detector based Hodoscope are dark current, efficiency, noise rate, strip occupancy and cluster size. RPCs having double gaps running modes is studied to control the quality of the chamber performance. The RPC consists of double gaps (two single gaps putting one on top of the other) and copper strips in the middle with common read-out. In our experiments, the signal is induced in the gaps by the two avalanches simultaneously leading to an improved detection efficiency being the sum of two single gap signals. Copper foils with signal cables (50 ohm impedance) are used to connect read-out strips to Front-End Boards (FEB) as also reported in reference 50 [50].

The data read form output of FEB in LVDS signals after amplification and discrimination, are further processed by the data acquisition system (DAQ). In our case, the DAQ consists of one VME crate housing twenty different modules. The 64-channels BARI TDC (Time to Digital Converter) sampled by a 40MHz clock corresponds to 25 ns time sensitivity. Each TDC processes the LVDS signals coming from four FEBs, which is an equivalent process protocol as implemented at Technion experiment [51].

TDCs are programmed in a "common stop" mode. When the trigger arrives from the NIM based signal using scintillators detectors, the data is transmitted to a PC for storage and analysis. PC stores all data in text file. Our new DAQ system converts these text file


into xml file because the size of text file depend on the event taken from the RPC. Minimum sizes for 10,000 events are 20 to 25 MB. When we analyze these data on-line we need minimum size of files. After conversion of these files into "xml" we use JAVA program to draw plots of strip occupancy, efficiency and cluster size. Dark current is also measured on-line for each detector. The results on each quality output check are discussed below:

4.2 Strip Occupancy Plot

Strip response profiles are created and they serve two main purposes: first, to ensure that the chamber is connected properly to the DAQ system and second, to ensure all readout strips are active and working properly as they are supposed to. Improper soldering of connections can lead to strips that appear to be dead in strip response profile. Each RPC contains total number of 96 readout strips and each of them is supposed to be in proper working condition. There can be some noisy strips, which show large number of hits and there can be some dead strips also, which show no signal or hit. Normally strip's resistance is 50 Ω and each strip draws about 5 μA current on the average. In this way all the strips of RPC are checked and faulty strips are observed. If chamber has more than 2 noisy or dead strips, then chamber is rejected and reassembled to remove this noisy and/or dead strip so that it can fulfill the CMS requirement. We tested a large number of chambers. The plots of strip occupancy for the chambers CMS-RE-2/2-PK-032 and CMS-RE-2/3-PK-015 at 9.4 kV are shown in Fig. 4.1 and 4.2 respectively. These plots are taken at 9.4 kV. In these plots there is no dead strip except the strip number 32, which is noisy. It is due to the high voltage cable which is passing near this strip.

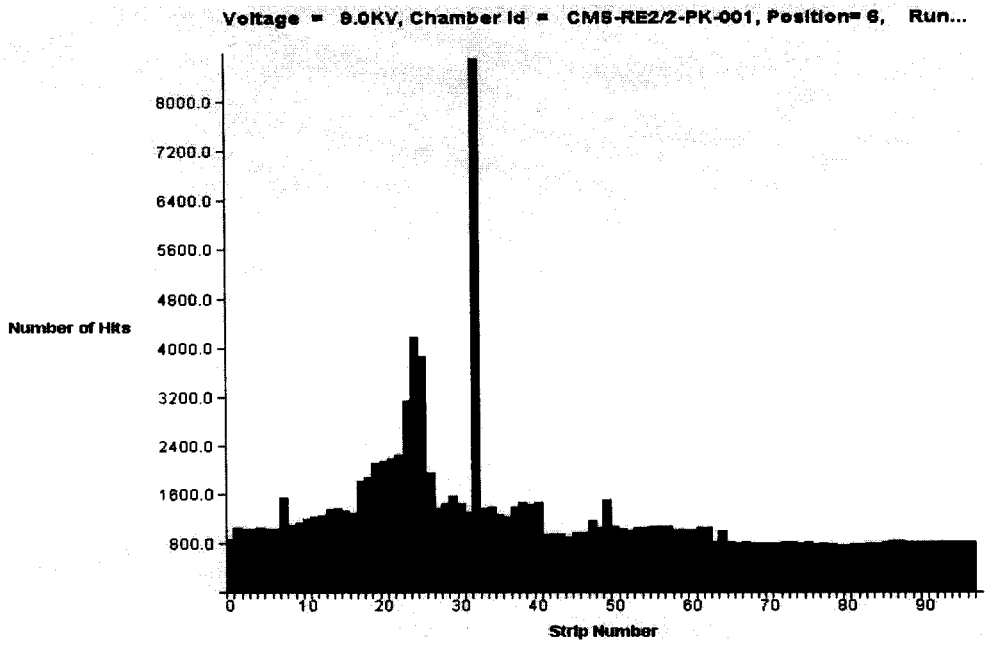

Fig. 4.1 Strip Occupancy Plot

4.3Efficiency

The RPC detector efficiency is obtained with the "coincidence" method by evaluating the ratio between the number of events in which RPC has at least one fired strip in the trigger window (100 ns) and the total number of recorded events, with correction for spurious hits [52].

The efficiency is defined as

$$\varepsilon = \frac{[(N_{ob}/Nt) - Ps]}{1 - Ps} \times 100 \qquad \text{Eq: 4.0}$$

Where N_{ob} is the number of observed events. N_t is the number of total events and P_s is the probability of the spurious hits. The probability of the spurious hits is determined by counting the hits in a time window delayed 100 ns after the trigger. The value of the efficiency should be greater than 95% at operating voltages and the efficiency plateau starts at 9.5 kV. For good performances of RPC, its efficiency plateau should lie in the range of 300 V. The maximum efficiency and length of plateau depends upon the gas mixture. The efficiency plots of the chambers CMS-RE-2/3-PK-044 is shown in Fig 4.2. When the voltage is small, the ionization in the chamber is small which results in small current in the gap. As we increase the voltage, efficiency also increases, which shows that the ionization in the gap is more and chamber draws more current. After the 9.2 kV the behavior of efficiency is linear. The operating voltage starts 9.2 kV to 9.6 kV and operating plateau is greater than 300 volts. The value of efficiency is almost > 95% at high voltage

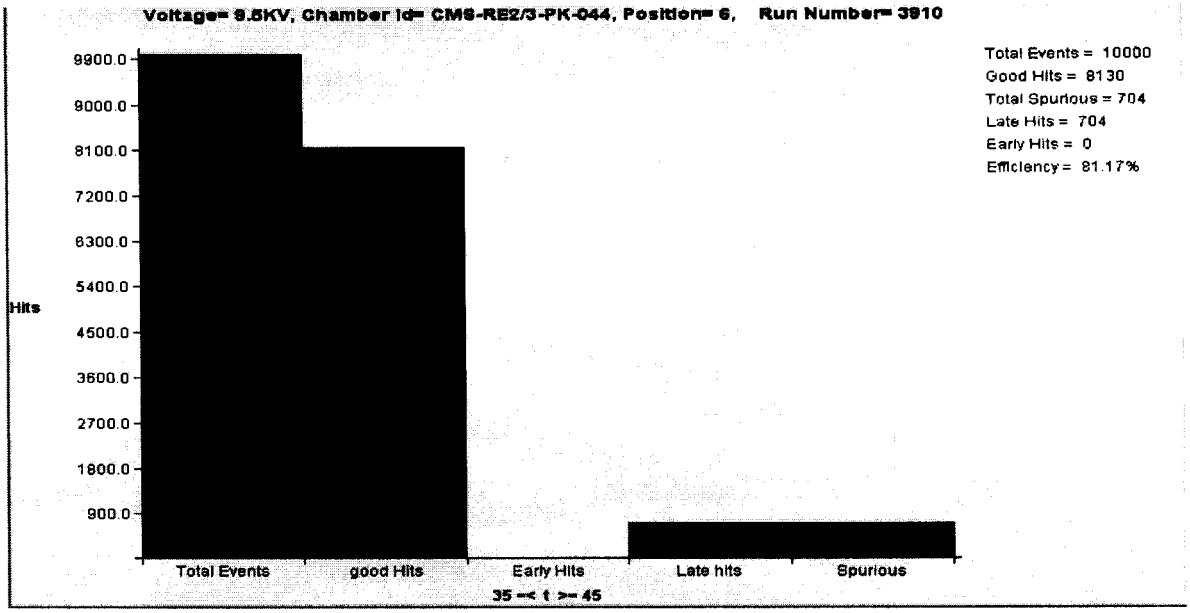

Fig. 4.2 Efficiency Plot of RPC

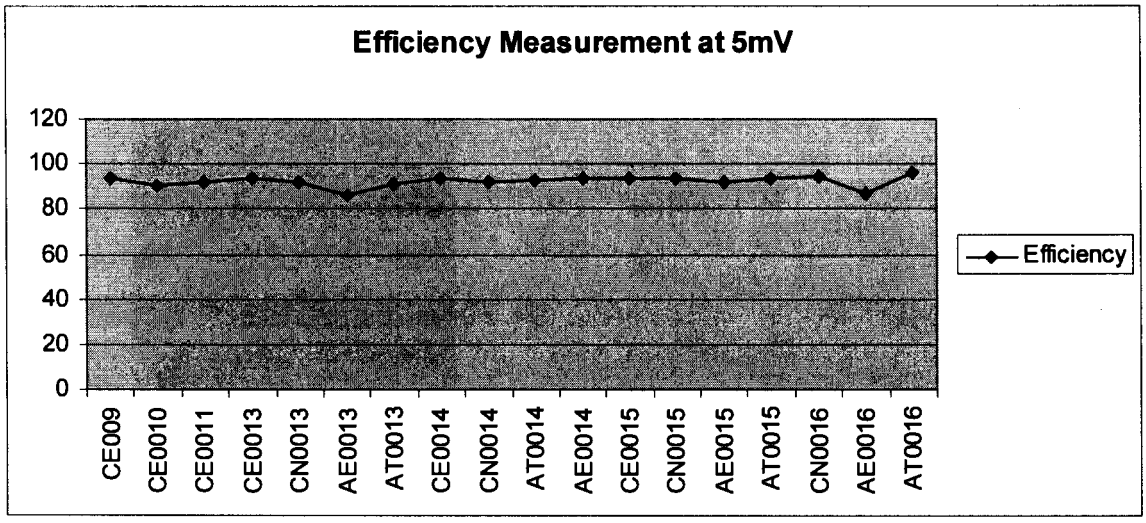

Fig. 4.2.1 Efficiency Plot of Scientillator

4.4 Cluster size

Another important parameter of chamber performance is the cluster size. This is measured for every chamber at several voltages. A hit is defined as a signal recorded on a single readout strip. To define a cluster, we first ordered in time all the hits of a particular RPC and then search for clusters. The cluster size of a chamber is defined as "the average value of the cluster size distribution, sampled in the first 25 ns of the trigger window (100 ns)". A cluster size ideally should be small in order to achieve the required resolution. Keeping the CMS criteria in view, the efficient performance of the RPCs should be less than three hits per strip. The cluster size can be reduced by changing the Front-End electronics thresholds to optimal value, as earlier tried in one of the CMS experiment [53]. The plots of the cluster size for the chambers CMS-RE-2/2-PK-002 is shown in Fig. 4.3.

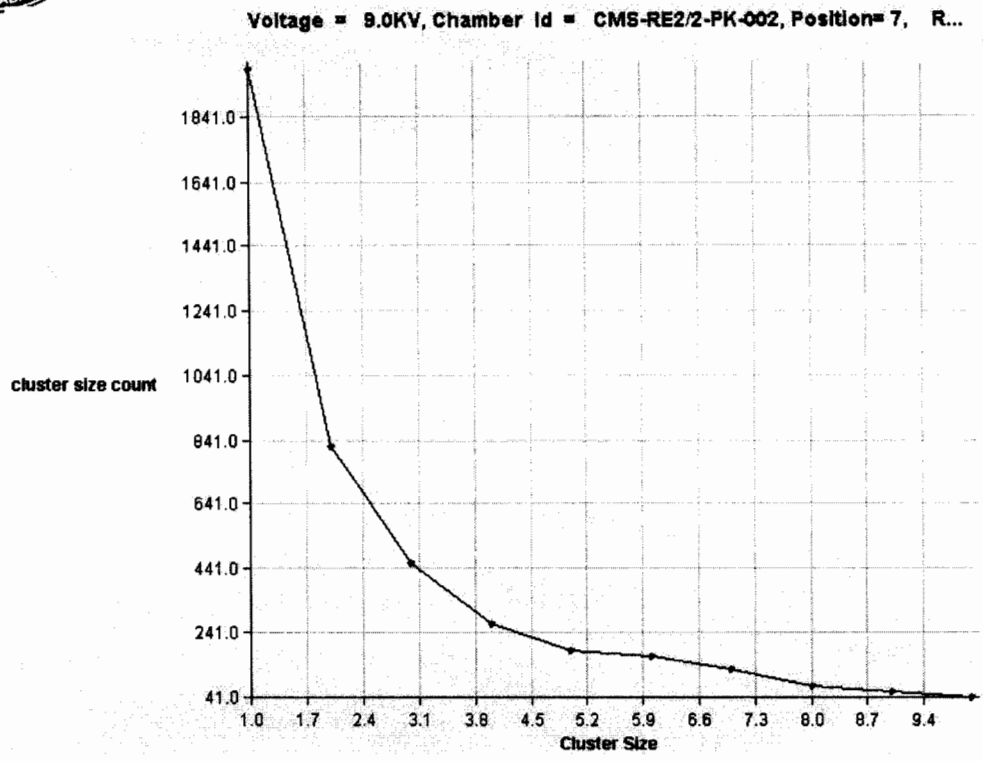

Fig. 4.3 Cluster size

If we look at this plot the cluster size is less than three. So we can say that both the plots are in good agreement as defined in CMS criteria. The formation of clusters from 8.6 kV to 9.6 kV is not uniform, it grows with the increase of the high voltage, this explains the requirement of threshold voltage consumption in this experiment.

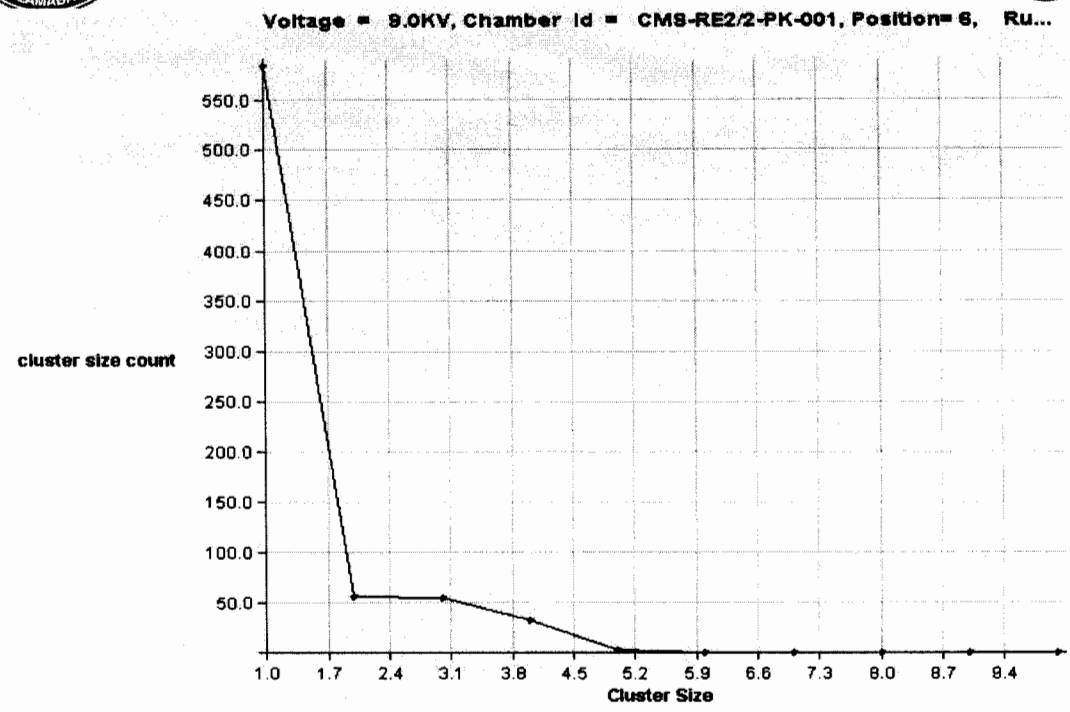

Fig. 4.4 Timing windows/Hit frequency

4.5 The Hardware-Software Integration analysis

The main window consisted of two split panels. One on the left contains the run number and all the RPCs that are tested during that run. Right panel contains different graphs that were obtained after running the online analysis.

On top there is a menu bar which has different options to analyze data. At the bottom there is a status bar which has information about the current status of the software. A user could select a desired chamber number and applied voltage value from a drop down list. As soon as the value of applied voltage is selected by the user, DAQ starts to process the corresponding data residing on the web server. After processing, a user could see graphs of the following types:

• The strip occupancy plot

• Cluster size of a chamber plot

A user could define the values for the time windows for the good hits and also for the spurious hits. In future we are looking to include the simulation of the chambers and hit profile to observe the chambers in a visual manner.

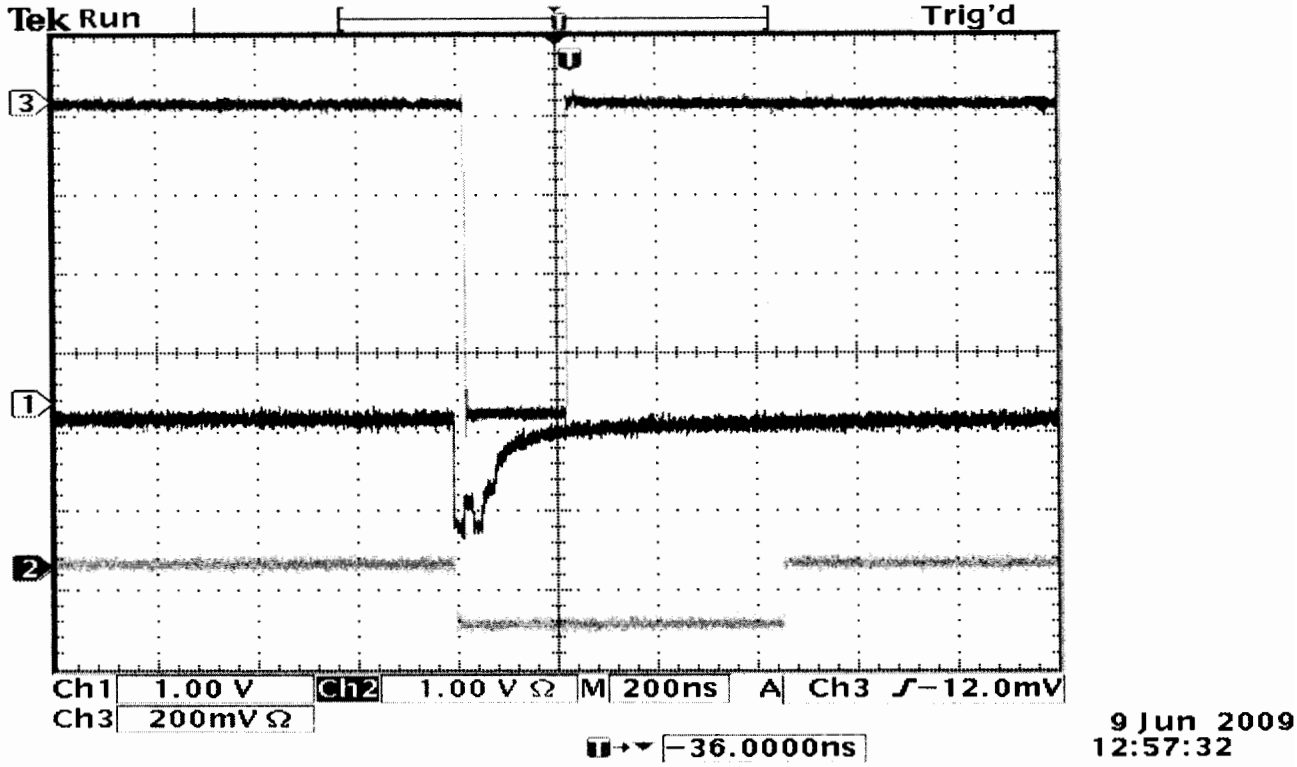

Fig 4.5 on-line scintillator output on Oscilloscope of real data

4.6 CAEN Power Supply Interface-An operational aspect of Hodoscope

In our experiment, the control of CAEN Power Supply systems contains a software interface independent of the Power Supply models and of the communication path used

to exchange data with them at present. CAEN provides the CAENHV Wrapper.lib for Microsoft JAVA Win32 DLL. The Linux dynamic library CAEN HV Wrapper is logically located between an application like Active HV or OPC server and the lower layer software libraries, as shown in the Fig.4.5.

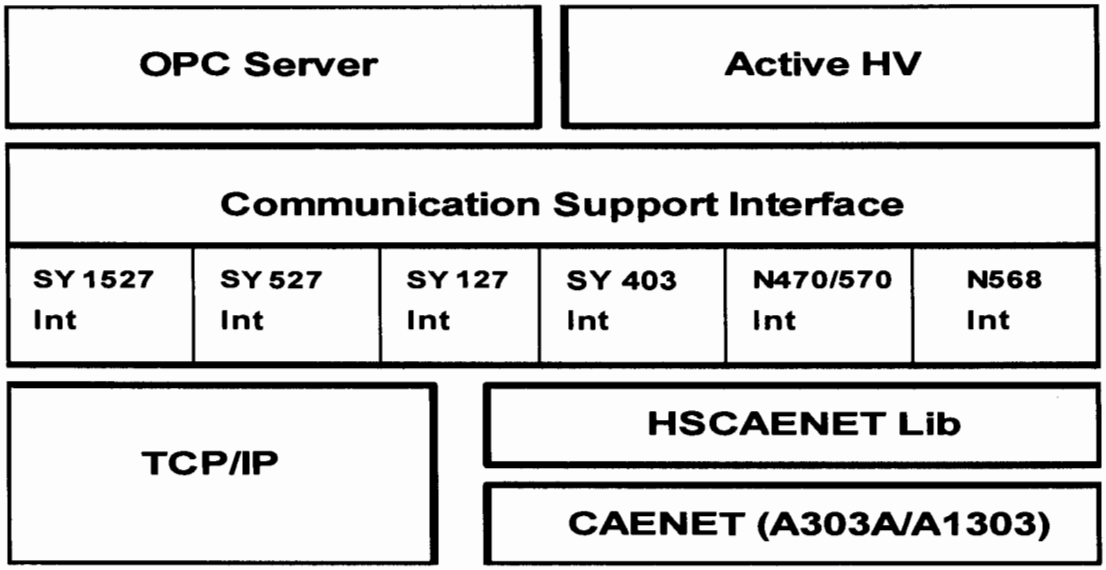

Fig. 4.6 Active HV or OPC server

The user of the library must identify the Power Supply to which to connect by choice of a string, like "SY1527", "SY527", "System0", or any other value the user prefers because each has different logical address. Once the Communication Support Interface establishes that the given Power Supply is a CAEN SY1527, it calls the specific functions of the SY1527 Interface which, on his side, uses the standard socket interface to control the Power Supply. This is achieved in this fashion during our experiments. If the string identifies a CAENET controllable Power Supply, the CAEN HV Wrapper calls the procedures in the relevant interface. Recently, it prepares the correct CAENET packet to pass to HSCAENETLib.

If link type is TCPIP, it executes a login command to power supply and, if it works well, it executes the command which returns the system model name like SY1527 to see which type of high voltage system is connected. This is absolutely in line with other result reported in lecture for such operations [Table 2.1]. An example of such action is shown in Fig 4.6, where a visual is scanned form of our designed hodoscope.

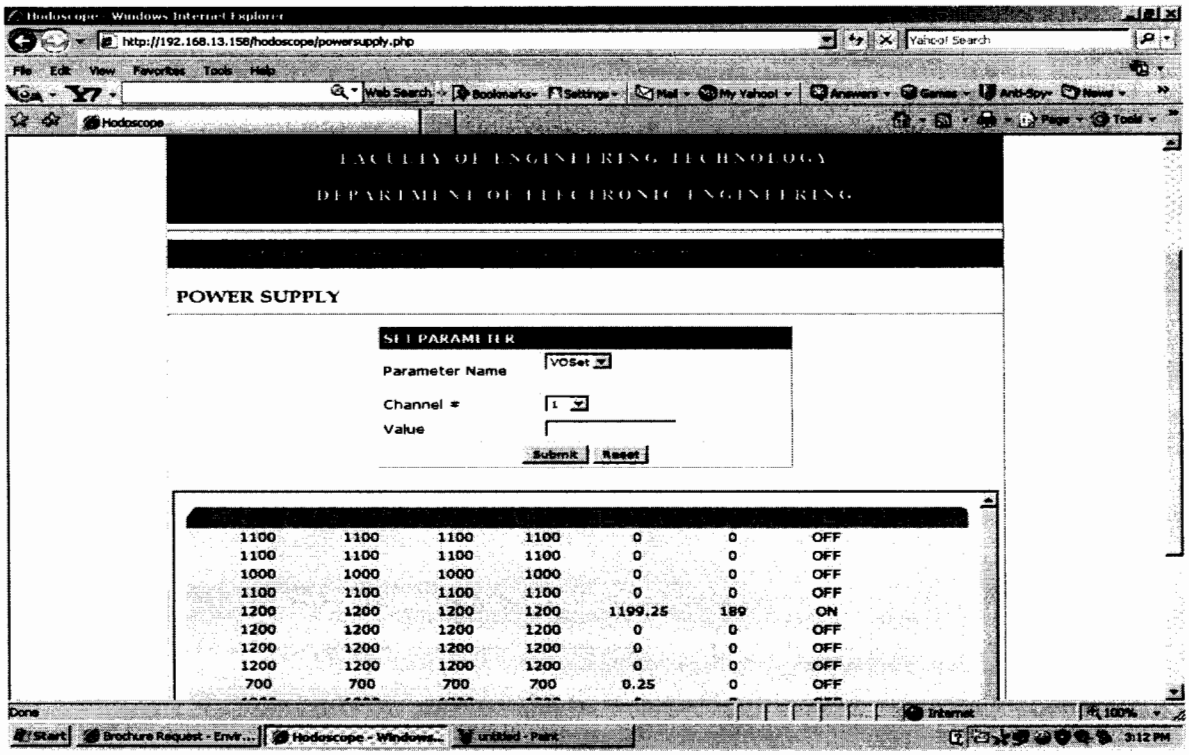

Fig. 4.7 Online Power supply Visual

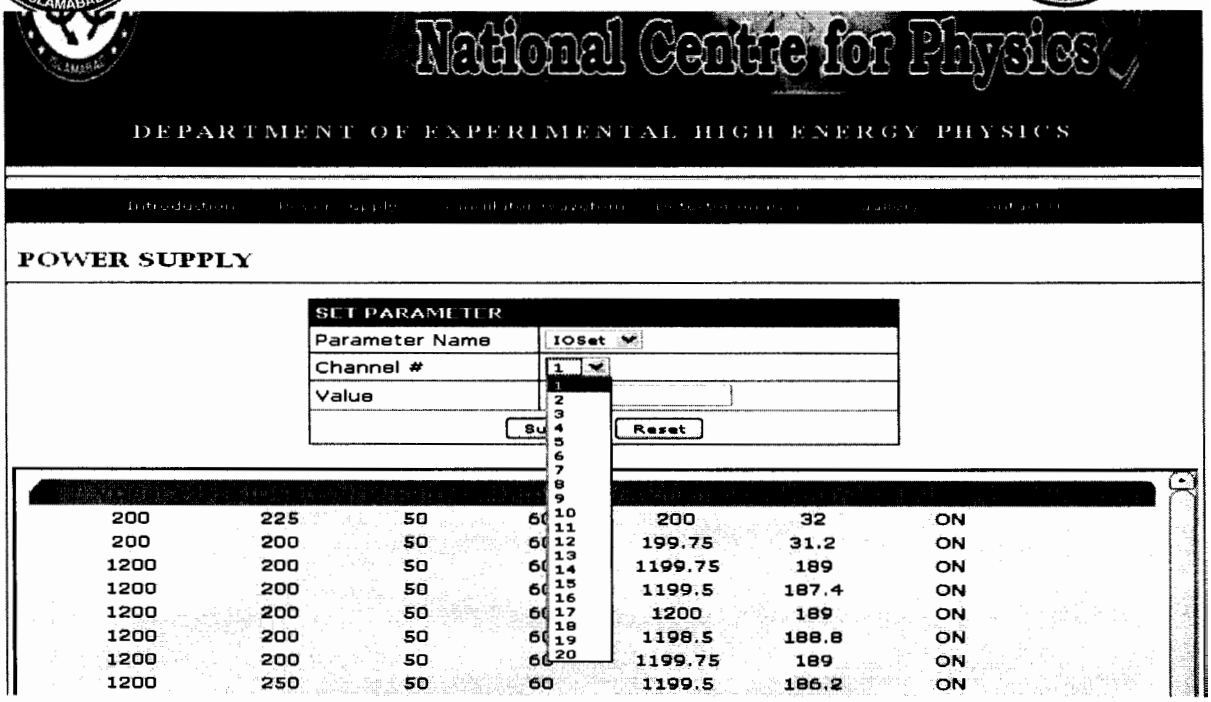

Fig. 4.8 Online Power supply channel selection

Chapter 5

Conclusion and Future Work

5.1 Introduction

In this regard we have carefully designed the working condition of the experiment such as setting up threshold of scintillators, usage of optical grease and generation of fine trigger form the scintillator. We have successfully developed the mode to translate the result online for further use and tested them against the CMS criteria. To meet the criteria of CMS; we have designed, developed and calibrated a hodoscope at NCP National Centre for Physics at Islamabad to test RPCs.

The result shown in previous chapter reveals that end cap RPCs meet all the CMS criteria. Therefore; they are suitable for the installation in CMS detectors. In order to be able to use the RPCs arranged in the double gap structure on the basis of muon triggering system for the CMS detector all of them must qualify the testing criteria. This is qualified using our developed protocols for online cosmic rays hodoscope. These RPCs may be processed for man production, one needs to make sure, that they are as simple and cheap as possible without compromising on their performance and they should complete the CMS requirements which are imposed on the RPCs. The CMS criteria tested against our hodoscope is:


- Efficiency should be >= 80 - 95%
- Cluster size should be < 3
- Dark current should be < 5 μA
- Strip occupancy should be < 3 noisy or dead strips

If any chamber does not fulfill these requirements then chamber is not accepted and sent back to remove that problem. In our experimental results all the parameters of RPC has been fulfilled against the ones imposed by the CMS criteria. Since, last one and a half year, we have tested around 90 Endcap Resistive Plate Chambers including their initial tests (gas leakage, HV etc) and finally the cosmic test. For monitoring dark current and high voltage of the detectors, we control HV power supply and monitor all parameters remotely on web using our developed hodoscope.

After testing, they may be shipped to CERN, where they will be installed in the CMS experiment at LHC, which will again run in 2010.

Future work

1. The objective of design is shown waveform pattern on the oscilloscope but channels of Oscilloscope is only four one for top layer second for bottom layer and third for Coincidence of both layer forth is Scintillator output. The board is select one Scintillator from sixteen different Scintillator using RS-232 ports. The

Multiplexer and Universal Asynchronous Receiver and Transmitter (UART) implemented in FPGA the select one Scintillator from sixteen inputs. The method is to interface a laptop or PC with an FPGA kit using RS-232 port on the board with appropriate interactive signals.

2. The lifetime of cosmic ray muons is measured by observing signals from an incoming muon and its decay electron in a block of Scintillator.

   The apparatus consists of a wooden box containing a block of plastic Scintillator and a photomultiplier tube (PMT). Light produced when cosmic rays pass through the Scintillator is detected by the photomultiplier. Occasionally a cosmic ray muon stops in the Scintillator resulting in two signals within about 10 microseconds - the first from the incoming muon and the second from the decay electron. The time delay between the two signals is measured and passed to a Personal computer. This technology needs an improved. Further research and development may be required to differentiate between two distinct lifetimes so that quality assurance may be conducted on the online hodoscope.

Reference:

Web reference
[1].http://innovexpo.itee.uq.edu.au/2008/projectDetails.html?offering=52&student=s4076728

[2]. Waqar Ahmed. et al, CMS-NOTE-2008-031, CERN-CMS-NOTE-2008-031.-Geneva: CERN, 2008(CERN-note), (2008), P#1

[3]. Waqar Ahmed. et al, CMS-NOTE-2008-030; CERN-CMS-NOTE-2008-030.-Geneva: CERN, (2008) P#1.

Web Reference
[4] http://www.aurelia-micro.it/nuclear/download.php?id=122&obj=M

[5]. M.Abbresciaa, et al, (CERN-note),P#1 2006.

Web Reference
[6]. http://hyperphysics.phy-astr.gsu.edu/hbase/astro/cosmic.html.

[7] K. Hagiwara et al., "The Review of Particle Physics", Phys. Rev. D66, (2002), P#1.

Web reference
[8] http://www.phys.ufl.edu/reu/2002/reports/munoz.pdf

[9].Bressani, Tullio, et al, Nuclear science, IEEE transactions volume 31, issue 1,(1984) P#136

Web Reference
[10] http://www.phys.ufl.edu/reu/1999/reports/wilson/wilson.pdf

[11]..Arba.M, et al, Nuclear science symposium and medical Imaging conference, IEEE Conference record. Volume 2, (1994) P#603

[12].Oluwaseun Amoda, "Research and development on RPC Detectors & design and construction of a cosmic ray test stand", Electrical Engineering Department, The University of Memphis, TN 38152. (Thesis), P#1

[13].G.laselli et al., "Study of detailed geometry of barrel RPC Strips", CMS Note 2000/044,(CERN-note),(2000), P#1

Web Reference
[14] http://bimasakti.fizik.um.edu.my/fzu/sumber/muonlab.pdf

[15].K.Banzuzi, et al., CMS IN-2000/043. (CERN-note), (2000), P#1

Web Reference
[16] http://www.aurelia-micro.it/nuclear/getattach.php?mod=N840&obj=mn

[17].Corrin D. Wilson, "CMS End cap Muon Chamber Testing". Department of Physics, old Dominion University, Norfolk, VA 23508; Andrey Korytov. Department of Physics. University of Florida, Gainesville.F132611. (Thesis)

[18].J.A.Munoz, "Scintillators as an External Trigger for Cathode Strip Chambers" Department of Physics, Princeton University, Princeton, NJ 08544.(Thesis)

[19].R.Santonico, Nuclear Instr and meth, (1981) ,P#377.

[20].C.Albajar et al., Nuclear Instr and meth, (2004), P# 465.

[21].S.H. Ahn et al., Nucl. Instr.and Meth, (2001), P#323.

[22].I Crotty et al., Nucl.Instr.and Meth, (1993), P#133.

[23]. Giuseppe et al., TDC RPC V2.0- DE ROBERTIS-INFN BARI 28.05.2003. (CERN-note)

Web Reference
[24] http://www.caenaerospace.it/nuclear/product.php?mod=N840

[25]. Y.Ban, et al., CMS Note, (CERN-note), (2004),P#1

Book Reference

[26]. William R.Leo, "Techniques for Nuclear and Particle Physics Experiments", Second Revised Edition, 1994-02-25 ISBN: 3540572805

Web Reference
[27]http://faculty.washington.edu/~wilkes/salta/talks/Gsnow_scintillator_lesson_files/slide0002.htm

Thesis reference
[28].Oluwaseum Amoda, "Research and Development on RPC detectors & Design and Construction of a Cosmic Ray Test Stand", Electrical Engineering Department. The University of Memphis. TN 38152 (Thesis)

Web Reference
[29] http://www.dailygalaxy.com/my_weblog/particle_physics/

[30]. The CMS Collaboration, The Hadron Calorimeter, Technical Design Report, CERN/LHCC 97-31, CMS TDR 2, 1997

[31]. The CMS Collaboration, The Electromagnetic Calorimeter, Technical Design Report, CERN/LHCC 97-33, CMS TDR 4, 1997

[32] The CMS Collaboration, The Tracker System Project, Technical Design Report, CERN/LHCC 98-6, CMS TDR 5, 1998

[33] The CMS Collaboration, Addendum to the CMS Tracker TDR, CERN/LHCC 2000-016, CMS TDR 5 Addendum 1, (2000), P#1

[34] R. Tenchini, Status of CMS, Nuclear Physics B - Proceedings Supplements Volume 156, Issue 1, June 2006, Pages 87-92

[35]. Y. Gernitzky et al, The Cosmic Ray Hodoscope for Testing Thin Gap Chambers at the Technion. ATL-MUON-2003-005, 25 July 2003, page# 01

[36] The CMS Collaboration et al., Cosmic ray tests of double-gap resistive plate chambers for the CMS experiment, PUBLISHED BY IOP PUBLISHING FOR SISSA, PUBLISHED: March 19, 2010

[37] T. Angelov, et al., Test set-up for the CMS resistive plate chambers, (2002) P#73.

[38] L.I.Dorman, "Cosmic Rays in the Earth's Atmosphere and Underground", The Netherlands, (2004), P#10, 340.

[39] L.I.Dorman, "Space Weather and Dangerous Phenomena on the Earth: Principles of Great Geomagnetic Storms Forecasting by Online Cosmic Ray Data", (2005), P# 2997

[40] Angelov 1 et al, Muon Telescopes at Basic Environmental Observatory Moussala and South-West University – Blagoevgrad, (2008),Sun and Geosphere, 2008; 3(1):P# 20 - 25

[41]. CMS Collaboration, "CMS: Muon Technical Design Report", P#1.

[42] Leprince-Ringuet, et al, "Cosmic Rays", (1950), Irish Astronomical Journal, Vol. 1, P#.159

[43] Garc´ıa-Ferreiralet al, Data acquisition system and event display for a hybrid silicon-scintillation detector, 2006 J. Phys.: Conf. Ser. 37 1 P#1-4

[44]. Dr. C.N. Booth, Scintillation Counters, PHY311/312 Detectors for Nuclear and

Particle Physics, P#1-5

[45] Corrin D. Wilson, "CMS Endcap Muon Chamber Testing", Department of Physics,

old Dominion University, Norfolk, VA 23508,P#1-12

Web reference
[46]. http://www.caen.it/nuclear/product.php?mod=SY1527

Projrct thesis
[47] J. A. Muñoz, "Scintillators as an External Trigger for Cathode Strip Chambers", Departmentof Physics, Princeton University, Princeton, NJ 08544.

Web Reference
[48].http://www.caen.it/nuclear/Printable/data_sheet.php?mod=N842&fam=nim&fun=disc

[49]. Katharina Breitenecker et al, science Direct Volume 67, Issue 12, December 2009, Pages 2088-2091

[50]. G. Carboni et al, A model for RPC detectors operating at high rate 2009 IOP Publishing Ltd and SISSA, P# 1-13

[51]. M. Abbresciaa et al, Science Direct Volume 550, Issues 1-2, 11 September 2005, Pages 116-126

[52]. E. Etzion et al,The Cosmic Ray Hodoscopes for Testing Thin Gap Chambers at the Technion and Tel Aviv University ATL-MUON-2003-005,25 July 2003

Web Reference
[53]. http://wiki.apache.org/ws/FrontPage/Axis/AxisGeneral

[54] Borislav Pavlov on behalf of the CMS RPC Barrel Collaboration, CMS BARREL RESISTIVE PLATE CHAMBERS - Physics in Collision - Zeuthen, Germany, June 26-28, 2003

Web Reference
[55] http://neutronm.bartol.udel.edu/catch/cr1.html.

Appendix

An Overview of the LHC

One of the main events in the field of particle physics is the construction of the Large Hadron Collider (LHC). This machine is being installed into the existing Large Electron Positron (LEP) tunnel at the European Centre for Nuclear Research (CERN) laboratory across the Franco- Swiss border west of Geneva, Switzerland. The pre-existence of the LEP tunnel and of the CERN accelerator chain for particle injection makes the cost of the machine affordable. The LHC will be the largest hadron collider in the world and will extend the energy frontier of physics, offering a further insight into the basic mechanisms of nature, as for example the mechanism that gives masses to the fundamental constituents of matter.

LHC is a very challenging project because of the engineering constraints and the physics requirements. As a consequence of the fixed length of the ring, imposed by the choice of using the existing LEP tunnel, the limit to the acceleration of the colliding particles comes from the strength of the maximum bending magnetic field. A new generation of superconducting magnets will provide the magnetic field necessary to achieve the TeV energy range. A large cryostat will keep the magnets at the working temperature of 1.9 K. The statistical significance of the scientific results will be obtained by means of the exceptional luminosity of LHC, which will ensure a good number of interesting events per year. On the other hand, it will lead to a very high radiation environment for the

particle detectors. Therefore, the survival of the detectors in this harsh radiation environment during 10 years of operation planned for the machine is a challenging issue for the detectors.

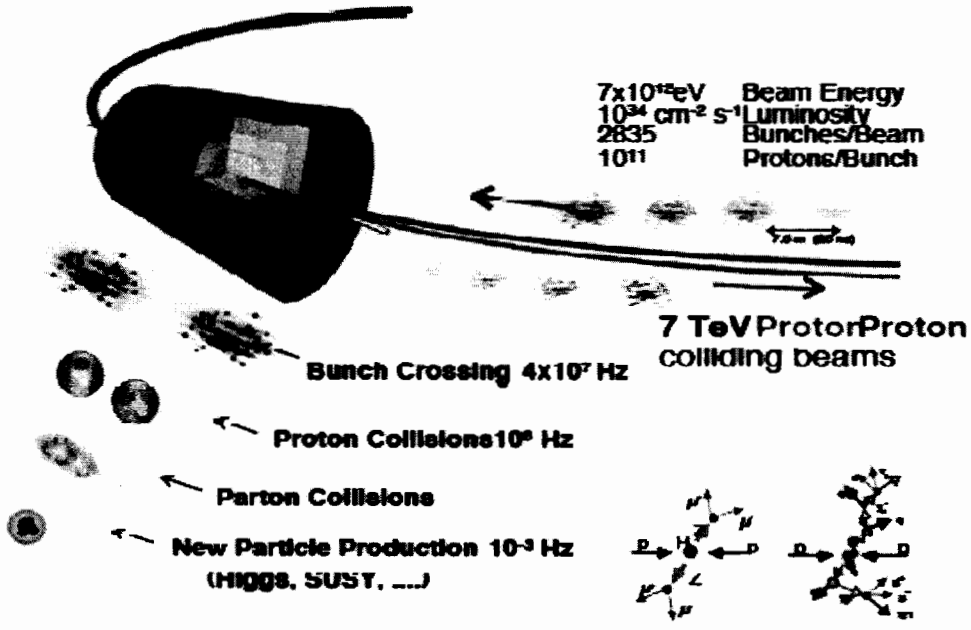

Figure 1-1: Collisions at the LHC.

1.1 The Large Hadron Collider

The LHC is a two-ring machine with a total length of 27 km, lies on an average of 100 m


below ground between Lake Geneva and the Jura mountains, which will allow the head-on collision of proton beams, shown in Fig. 1-1, each with an energy of 7 TeV, and beam collisions of heavy ions, such as lead, with a total collision energy in centre-of-mass of ≈ 1, 250 TeV, about thirty times higher than the Relativistic Heavy Ion Collider (RHIC) under construction at the Brookhaven Laboratory in the US. Joint LHC/LEP operation could supply electron-proton collisions with a centre-of-mass energy of 1.5 TeV, some five times higher than presently available at HERA in the DESY Laboratory, Germany. The research, technical and educational potential of the LHC and its experiments are enormous. The wide range of physics possibilities will enable LHC to retain its unique place on the frontiers of physics research well into the next century.

A TeV is a unit of energy used in particle physics. 1 TeV is about the energy of motion of a flying mosquito. What makes the LHC so extraordinary is that it squeezes energy into a space about a million million times smaller than a mosquito [1].

The LHC is an accelerator, which will allow scientists to penetrate still further into the


energy E the luminosity of a collider (a quantity proportional to the number of collisions per second) should increase in proportion to E2. This is beacuse the De Broglie wavelength associated to a particle decreases as 1/E and hence the cross section of the particle decreases as 1/E2. At LEP the luminosity culminates around L = 1032 cm−2 s−1, whereas in the LHC it will reach L = 1034 cm−2 s−1. This value will be obtained by filling each of the two rings with 2835 bunches of 1011 particles each, the resulting large beam current (Ib = 0.53 A), injected in the LHC by the Super Proton Synchrotron (SPS) at the energy of 0.45 TeV. The bunch spacing will be 7.48 m, corresponding to an interval between two successive bunches of 25 ns at the collision energy.

A 8.36 Tesla magnetic field, over five times those used a few years ago at the SPS proton anti proton collider, and almost 100, 000 times the earth's magnetic field, provided by 1296 superconducting dipole magnets over a total magnetic length of ≈ 15 km and the inner diameter of 56 mm [2], will guide the protons in the LHC orbits. Superconducting quadrupole correctors will make the orbit corrections to the spurious non-linear components of the guiding and focusing magnetic fields of the machine and allow the recovering of the required beam density after interactions. Special orbit correctors will be used, as sextupole, octupole and decapole magnets. The luminosity lifetime will be about 10 hours.

The two beam pipes of LHC and the superconducting coils will be hosted in the same Super fluid helium cryostat at the temperature of 1.9 K. 1.1.2 Physics at LHC The LHC machine and the planned experiments have been designed to study the extrapolation of

the present knowledge in particle physics to the LHC energy scale and to detect the signatures of a new and possibly unexpected physics above the TeV energy threshold. One of the main goals of LHC is the discovery of the associated gauge boson, the Higgs particle. The limits of the Higgs mass are set in the range 115 GeV < mH < 1 TeV, where the lower limit comes from the present electroweak data and the upper is theoretical. The experiments are designed to cover the different physics signatures of the Higgs, consisting in the identification of the predicted decay modes, with statistical significance over all the mass range. This requires very high luminosity because the cross section for heavy particle scales inversely with the square root of their masses. The rate of events is obtained by the product of the cross section and the luminosity. The rate of the Higgs boson production at the expected LHC luminosity and energy is $\approx 4 - 5 \times 10{-}3$ s−1, assuming the Higgs mass equal to 500 GeV.

1.2 The LHC Experiments

Four experiments, with huge detectors, will study what happens when the LHC's beams collide. They will handle as much information as the entire European telecommunications network does today.

As well as having the highest energy of any accelerator in the world, the LHC will also have the most intense beams. Collisions will happen so fast (800 million times a second) that particles from one collision will still be traveling through the detector when the next collision happens. Understanding what happens in these collisions is the key to the LHC's success.


The experiments are:

- ATLAS (A Toroidal LHC Apparatus)
- CMS (Compact Muon Solenoid)
- ALICE (A Large Ion Collider Experiment)
- LHCb (The Large Hadron Collider beauty Experiment)

In collaboration with CERN, Pakistan is working on the CMS experiment at the LHC. There are many different parts of the CMS experiment, but we are focusing on the endcap region of this experiment.

1.3 The CMS Experiment at LHC

The Compact Muon Solenoid is one of the two multi-purpose detectors foreseen for the Large Hadron Collider being built at the CERN. The CMS detector consists of several sub-detectors measuring energy, momentum, and charge of particles generated in collisions of proton beams with a centre of mass energy of up to 14 TeV.

1.3.1 Detector Overview

The CMS detector is designed to study proton-proton collisions as well as heavy ion collisions at the LHC. The cylindrical shape (see Fig. 1-3) is determined by the large superconducting coil generating a solenoidal magnetic field of 4 Tesla strength and by the iron return yoke.The yoke is divided into five wheels and a group of three endcap discs at each end of the detector. The magnet yoke is instrumented with muon detectors

while the tracking system (based on silicon pixel and silicon strip detectors), the electromagnetic calorimeter (ECAL, made

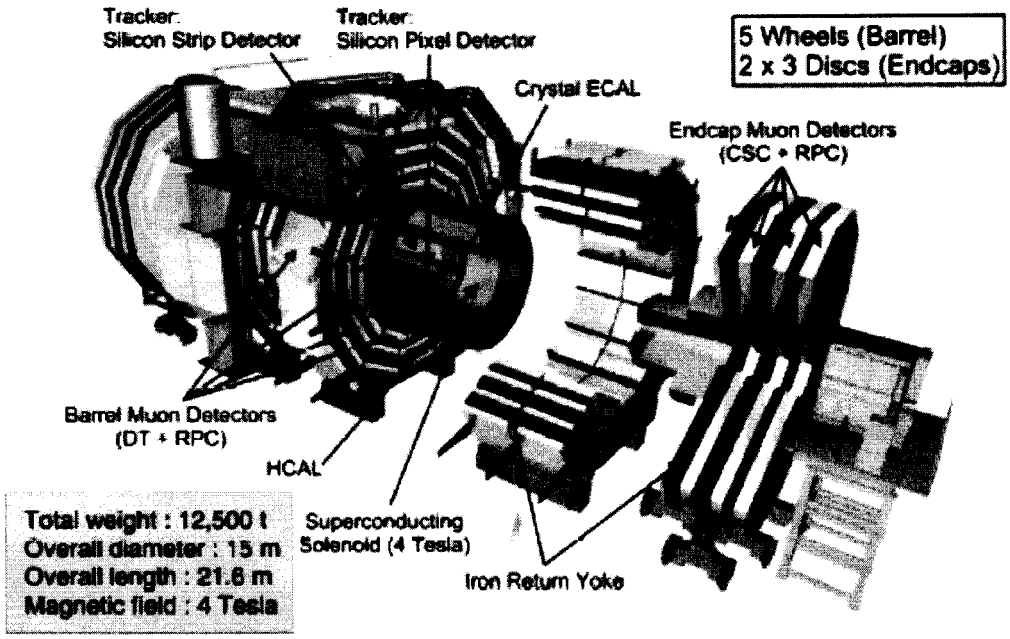

Figure 1-3: Artists view of the CMS detector.

of PbWO4 crystals) and the hadronic calorimeter (HCAL, made of copper plates interleaved with scintillators) are placed inside the magnet coil [3]. A schematic diagram of the CMS detector is shown in Fig. 1-4.

1.3.2 The Tracking System

A robust and versatile tracking system is of the utmost importance for an experiment designed to address the full range of physics which can plausibly be accessed at the LHC.

The CMS tracking system is designed to reconstruct high-PT muons, isolated electrons and hadrons with high momentum resolution and an efficiency better than 98% in the range $|\eta| < 2.5$. It is also designed to allow the identification of tracks coming from detached vertices. Such vertices arise from decays of b quarks, which provide very useful signatures for a broad spectrum of new physics. Visible particles are measured by the various sub-detectors and identified from their characteristic pattern as shown in Fig. 1-5.

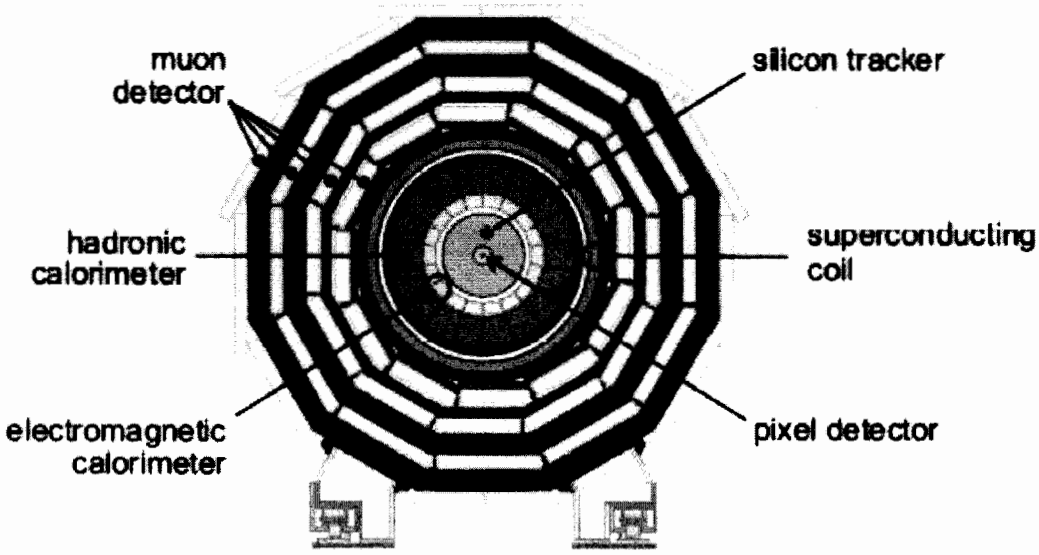

Figure 1.4: A schematic cut through the CMS detector.


1.3.3 The Electromagnetic Calorimeter

One of the principal CMS design objectives is to construct a very high performance Electromagnetic Calorimeter. A scintillating crystal calorimeter offers excellent performance for energy resolution since almost all of the energy of electrons and photons is deposited within the crystal volume. CMS has chosen lead tungsten crystals, which have high density, a small Moliere radius and a short radiation length allowing for a very compact calorimeter system.

1.3.4 The Hadron Calorimeter

The Hadronic Calorimeter, plays an essential role in the identification and measurement of quarks, gluons, and neutrinos by measuring the energy and direction of jets and of missing transverse energy flow in events. Missing energy forms a crucial signature of new particles, like the super symmetric partners of quarks and gluons. For good missing energy resolution, a Hadronic Calorimetry coverage to $|\eta| = 5$ is required. The HCAL will also aid in the identification of electrons, photons and muons in conjunction with the tracker, electromagnetic calorimeter, and muon systems.

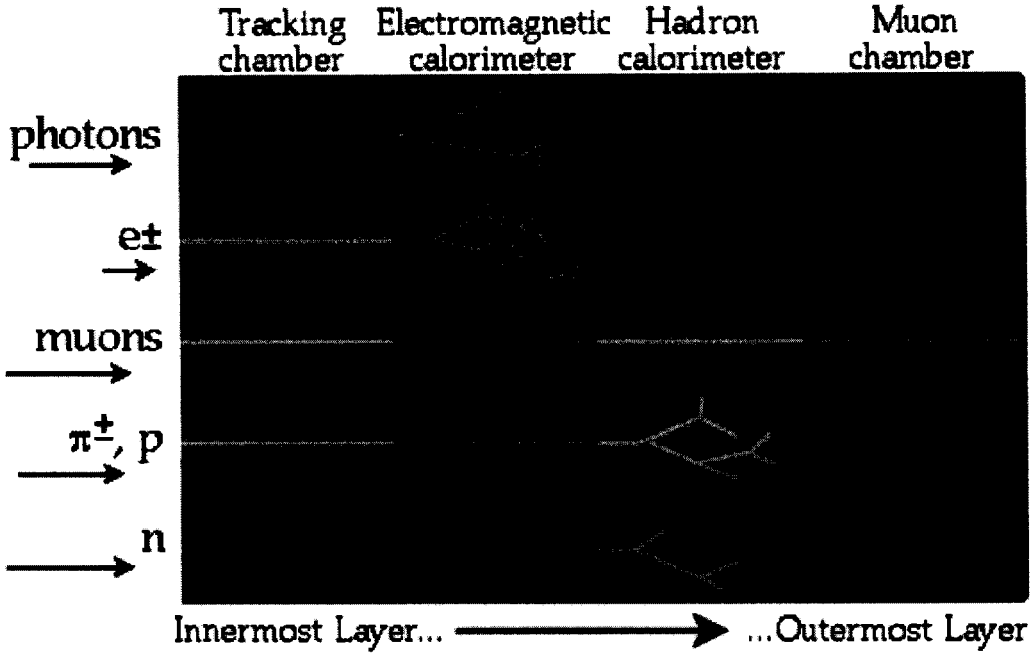

Figure 1-5: Energy deposited of different particles in different sub-detectors.

1.3.5 The Superconducting Magnet System

The CMS magnet system consists of a superconducting coil, the magnet yoke (barrel and endcap), a vacuum tank and ancillaries such as cryogenics, power supplies and process controls. The main parameters are the magnetic field of 4 Tesla, a yoke diameter of 14 m across flats, an axial yoke length including endcaps of 21.6 m. It will be the largest superconducting magnet system in the world: the energy stored into it, if liberated, will be large enough to melt 18 tons of gold [5].

1.3.6 Muon System

Muons are expected to provide clean signatures for a wide range of physics processes. The task of the muon system is to identify muons and provide, in association with the tracker, a precise measurement of their momentum. For the muon system 250 Drift Tube Chambers (DTs), 540 Cathode Strip Chambers (CSCs), and 912 Resistive Plate Chambers (RPCs) have to be built and installed. It is divided into two major parts (see Figs. 1-3 and 1-6):

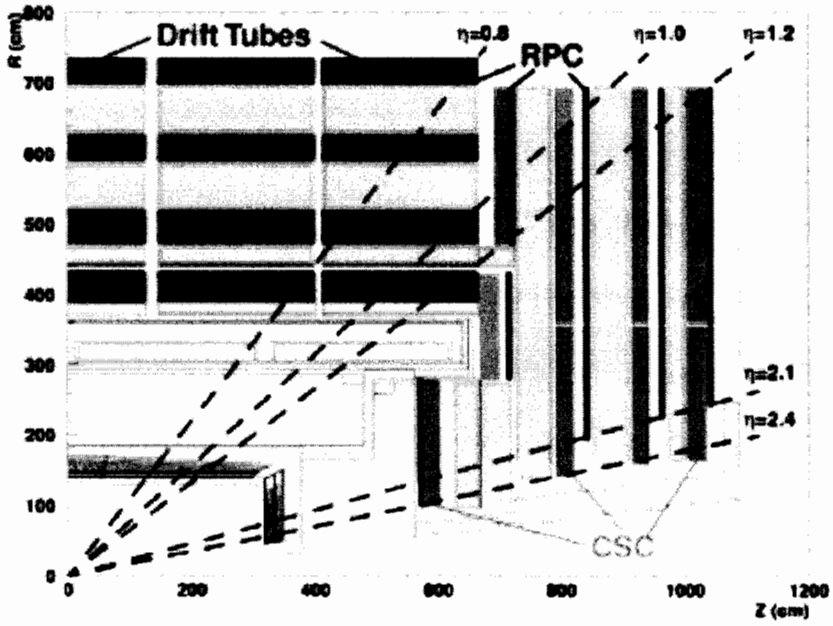

Figure 1-6: Cross sectional view of one quadrant of CMS showing the detectors of the muon system.

• barrel region ($0 < |\eta| < 1.2$): it consists of the five wheels instrumented with DTs and RPCs. The magnetic field is confined to the iron yoke plates. Within the muon stations the field is low and almost uniform. The expected muon rate is also relatively low: $R(\mu)$. 1 Hz/cm2. The neutron induced background is $1 - 10$ Hz/cm^2.

• endcaps ($0.9 < |\eta| < 2.4$): to cope with the strong and non-uniform magnetic field (up to 3.5 T) the endcap discs are instrumented with CSCs and RPCs. The muon rate is high at the order of $R(\mu)$. 200 Hz/cm^2. The γ and neutron induced background rate reaches values around 1 kHz/cm2 for large $|\eta|$.

1.3.7 Muon Detectors

CMS will use three types of gaseous particle detectors for muon identification: Drift Tubes, Cathode Strip Chambers and Resistive Parallel Plate Chambers. The DT and CSC detectors are used to obtain a precise measurement of the position and thus the momentum of the muons, whereas the RPC chambers are dedicated to provide fast information for the Level-1 trigger.The muon detectors are shown in Fig. 1-7.

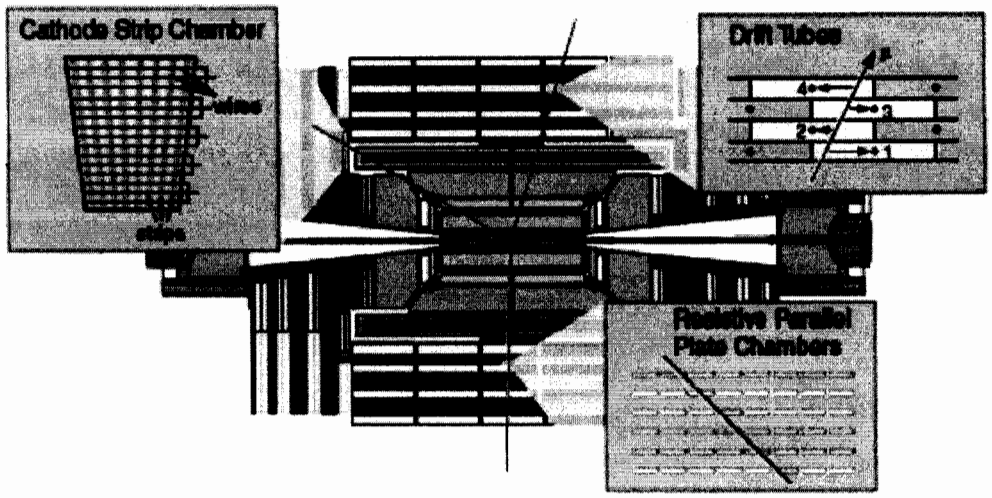

Figure 1-7: Muon detectors.

Drift Tube Chambers

The barrel region is instrumented with DT chambers. A muon chamber is built up from three so-called superlayers with four layers of half-a-cell width staggered drift tubes. When a muon passes through a DT cell it produces ionization along its track in the gas (the gas is a mixture of 85% Ar and 15% CO2). The primary generated electrons drift towards the anode wire in the centre of the cell. In the high electric field close to the wire, the gas amplification generates an electrical signal on the wire. The time needed by the primary electrons to reach the anode is measured. The spatial position of the track is calculated from the time measurement and the known time-to-distance relationship. To resolve the intrinsic left-right ambiguity of a single cell, it is necessary to exploit the